



**A SUMMARY REPORT ON STORE HEATING TECHNOLOGY**

**R. K. Matthews  
ARO, Inc., a Sverdrup Corporation Company**

**VON KÁRMÁN GAS DYNAMICS FACILITY  
ARNOLD ENGINEERING DEVELOPMENT CENTER  
AIR FORCE SYSTEMS COMMAND  
ARNOLD AIR FORCE STATION, TENNESSEE 37389**

**September 1978**

**Final Report for Period March 1977 to April 1978**

**Approved for public release; distribution unlimited.**

**Prepared for**

**AIR FORCE ARMAMENT LABORATORY/DLJC  
EGLIN AIR FORCE BASE, FLORIDA 32542**

## NOTICES

When U. S. Government drawings, specifications, or other data are used for any purpose other than a definitely related Government procurement operation, the Government thereby incurs no responsibility nor any obligation whatsoever, and the fact that the Government may have formulated, furnished, or in any way supplied the said drawings, specifications, or other data, is not to be regarded by implication or otherwise, or in any manner licensing the holder or any other person or corporation, or conveying any rights or permission to manufacture, use, or sell any patented invention that may in any way be related thereto.

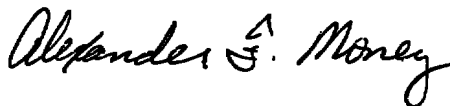
Qualified users may obtain copies of this report from the Defense Documentation Center.

References to named commercial products in this report are not to be considered in any sense as an indorsement of the product by the United States Air Force or the Government.

This report has been reviewed by the Information Office (OI) and is releasable to the National Technical Information Service (NTIS). At NTIS, it will be available to the general public, including foreign nations.

## APPROVAL STATEMENT

This report has been reviewed and approved.



**ALEXANDER F. MONEY**  
Project Manager, Research Division  
Directorate of Test Engineering

Approved for publication:

FOR THE COMMANDER



**ROBERT W. CROSSLEY**, Lt Colonel, USAF  
Acting Director of Test Engineering  
Deputy for Operations

# UNCLASSIFIED

REPORT DOCUMENTATION PAGE		READ INSTRUCTIONS BEFORE COMPLETING FORM
1 REPORT NUMBER <b>AEDC-TR-78-46</b>	2 GOVT ACCESSION NO.	3 RECIPIENT'S CATALOG NUMBER  1
4 TITLE (and Subtitle)  <b>A SUMMARY REPORT ON STORE HEATING TECHNOLOGY</b>		5 TYPE OF REPORT & PERIOD COVERED <b>Final Report - March 1977 to April 1978</b>
		6. PERFORMING ORG REPORT NUMBER
7 AUTHOR(s)  <b>R. K. Matthews - ARO, Inc.</b>		8. CONTRACT OR GRANT NUMBER(s)
9 PERFORMING ORGANIZATION NAME AND ADDRESS <b>Arnold Engineering Development Center/DOT Air Force Systems Command Arnold Air Force Station, Tennessee 37389</b>		10. PROGRAM ELEMENT, PROJECT, TASK AREA & WORK UNIT NUMBERS <b>Program Element 62602F Project 2567</b>
11. CONTROLLING OFFICE NAME AND ADDRESS <b>Arnold Engineering Development Center/DOS Air Force Systems Command Arnold Air Force Station, Tennessee 37389</b>		12. REPORT DATE <b>September 1978</b>
		13 NUMBER OF PAGES  <b>56</b>
14 MONITORING AGENCY NAME & ADDRESS (if different from Controlling Office)		15 SECURITY CLASS. (of this report)  <b>UNCLASSIFIED</b>
		15a. DECLASSIFICATION/DOWNGRADING SCHEDULE  <b>N/A</b>
16 DISTRIBUTION STATEMENT (of this Report)  <b>Approved for public release; distribution unlimited.</b>		
17 DISTRIBUTION STATEMENT (of the abstract entered in Block 20, if different from Report)		
18 SUPPLEMENTARY NOTES  <b>Available in DDC</b>		
19 KEY WORDS (Continue on reverse side if necessary and identify by block number) <b>external stores aerodynamic heating supersonic flow heat transfer wind tunnel tests</b>		
20 ABSTRACT (Continue on reverse side if necessary and identify by block number) <b>One of the problem areas associated with the supersonic carriage of external stores is concerned with temperature restrictions on critical components. Theoretical calculations were used to guide a two-phase experimental program which included both flight and wind tunnel testing. Flight heat-transfer measurements were obtained on a pylon-mounted BDU-12 at flight conditions of 40,000 ft and Mach numbers up to 2.5. The wind tunnel tests of a</b>		

## UNCLASSIFIED

# UNCLASSIFIED

## 20. ABSTRACT (Continued)

1/15-scale model included both pressure and heat transfer measurements on the flight test configuration plus several others. The results are discussed in three categories; wind tunnel, flight test, and correlation of wind tunnel and flight data. This work has clearly shown the flight capability for supersonic carriage of large stores and has demonstrated some of the available technology for defining thermal environments.

## PREFACE

The work reported herein was conducted by the Arnold Engineering Development Center (AEDC), Air Force Systems Command (AFSC), at the request of the Air Force Armament Laboratory (AFATL/DLJC) under Program Element 62602F. The AFATL Project Engineer was Major J. C. Key, Jr. The results of the test were obtained by ARO Inc., AEDC Division (a Sverdrup Corporation Company), operating contractor for the AEDC, AFSC, Arnold Air Force Station, Tennessee, under ARO Project Numbers V34A-06A and V34A-P8A. The manuscript was submitted for publication on June 28, 1978.

## ACKNOWLEDGMENT

The scope of the work presented in this report spanned many disciplines and organizations. The cooperation and communication between these organizations was one of the most satisfying aspects of this work. Particular thanks are due the following individuals: AFATL – Maj. J. C. Key, Jr., Mr. Charles Mathews; AFRPL – Mr. Lee Meyer, Lt. Mike Bond, Mr. Ed Zimmer; AFFTC – Mr. Bill Matthews, Lt. Col. Dostal; AEDC – Maj. K. B. Harwood, Mr. Alex F. Money, Mr. W. K. Crain, Mr. G. D. Spencer, Mr. L. L. Trimmer.

## CONTENTS

	<u>Page</u>
1.0 INTRODUCTION . . . . .	5
2.0 THEORETICAL CONSIDERATIONS . . . . .	7
3.0 DESCRIPTION OF EXPERIMENTAL PHASES	
3.1 Wind Tunnel Phase . . . . .	8
3.2 Flight Test Phase . . . . .	11
4.0 RESULTS AND DISCUSSION	
4.1 Wind Tunnel Phase . . . . .	13
4.2 Flight Test Phase . . . . .	15
4.3 Correlation of Wind Tunnel and Flight Test Data . . . . .	17
5.0 CONCLUSIONS . . . . .	19
REFERENCES . . . . .	20

## ILLUSTRATIONS

### Figure

1. Performance Envelope of Present-Day Aircraft . . . . .	23
2. Schematic Showing Extrapolation of Wind Tunnel Data to Flight Conditions . . . . .	23
3. AFRPL Project DAME Test Vehicle . . . . .	24
4. Photograph of Pylon-Mounted Store on F-111 . . . . .	24
5. Effect of Wall Temperature and Reynolds Number on Store Heating Rates . . . . .	25
6. Illustration of Extrapolation of Wind Tunnel Predictions to Flight Conditions . . . . .	25
7. Examples of Heating Data Obtained by Thermal Mapping Techniques (from Ref. 4) . . . . .	27
8. Comparison of Data Fairing with Interference-Free Calculations (from Ref. 4) . . . . .	29
9. Shadowgraph Illustrating Shock Impingement (from Ref. 4) . . . . .	29
10. Tunnel A Assembly . . . . .	30
11. Photograph of 1/15th-Scale Model of F-111 and BDU-12 in Tunnel A Test Section . . . . .	31
12. Photograph of Heat Gage BDU Model . . . . .	31
13. Photograph of GBU (outboard) and BDU (inboard) in Carriage Position on F-111 model . . . . .	32

<u>Figure</u>	<u>Page</u>
14. Configurations Tested in Tunnel A . . . . .	33
15. Illustration of Heat Gage Data Reduction Technique (Wind Tunnel) . . . . .	34
16. Photograph of BDU Nose with VKF Gages Installed . . . . .	35
17. VKF Instrumentation for BDU Aerodynamic Heating Test at Edwards AFB . . . . .	35
18. Flight Test Conditions . . . . .	36
19. Undisturbed (Interference-Free) Heat Distributions on BDU Model . . . . .	37
20. Heat-Transfer Results from Wind Tunnel (VKF/Tunnel A) . . . . .	37
21. Circumferential Heating Distributions . . . . .	38
22. Circumferential Pressure Distributions on BDU Model Mounted on Inboard Pylon . . . . .	44
23. Comparison of Measured and Calculated Interference Heating Distributions on BDU Model Mounted on Inboard Pylon . . . . .	44
24. Pre-Flight Photograph of BDU with Phase-Change Paint Applied . . . . .	45
25. Post-Flight Photograph of Phase-Change Paint after Mach 2.5 Flight . . . . .	46
26. Illustrations of Recorded $\dot{q}$ Variations (Noise) with Aircraft Parked in Hanger . . . . .	47
27. Illustration of Relative "Noise Level" for Flights . . . . .	48
28. Illustration of Data Reduction Technique (Flight) . . . . .	48
29. Heat-Transfer Results from Flight Test . . . . .	49
30. Principal Results from Flight Test No. 14 . . . . .	50
31. Illustration Showing the Importance of Ambient Temperatures on Maximum Possible Store Temperatures . . . . .	51
32. Comparison of Wind Tunnel and Flight Test Reynolds Numbers . . . . .	52
33. Comparison of Flight Test and Wind Tunnel Results . . . . .	53
34. Sketch Illustrating, Stand-Alone Airborne Data Recording System . . . . .	53

**TABLE**

1. Test Summary . . . . .	54
NOMENCLATURE . . . . .	55

## 1.0 INTRODUCTION

In 1957, Budemholzer, et al., documented a comprehensive study (Ref. 1) of the influence of pressure and temperature on the design of stores. To our knowledge, this was the first time store environments were investigated. Their work was primarily analytical and was based on flow-field solutions of stores exposed to a uniform free-stream flow (interference free). The subject of high-speed carriage of stores remained somewhat dormant until 1972 when Epstein (Ref. 2) presented a paper at the Store Compatibility Symposium defining the problems of supersonic carriage. According to Epstein, one important element preventing an expanded supersonic operational envelope comes from aerodynamic heating effects. Almost all present-day bombs and fuzes have, as their explosive charge, some form of TNT which melts at about 178°F. To avoid this possibility, the aircraft speed is restricted as illustrated in Fig. 1. Unfortunately, these limitations are imposed by somewhat arbitrary upper boundary temperature limits, since the determination of realistic store temperatures has been beyond the "state of the art." As Epstein pointed out, the complexity of the flow field defies analytical solutions, and flight testing every store is costly and impractical.

Epstein also addressed the question of developing some system of protecting the store (insulation) or of developing new explosives that will withstand extreme temperatures. But before this can be done we should first know to what temperatures the stores - and the critical components inside - will really, be subjected in flight. To do this analytically, one must know the following:

1. The recovery temperature (Fig. 1) and the length of time at a given flight condition,
2. The rate at which heat is being transferred to the store (i.e., the heat transfer coefficient,  $h$ ), and
3. The thermophysical properties of the store so that a heat conduction solution can be obtained.

Of these, the heat-transfer coefficient is the hardest to determine. However, within recent years, wind tunnel techniques have been developed to measure the heating distributions on pylon-mounted stores. These techniques are described in Ref. 3. The application of these wind tunnel results to actual flight conditions is discussed by Matthews, et al., in Ref. 4, and Fig. 2 is a schematic illustrating the main points of the extrapolation procedures. Determination of the proper aerodynamic scaling law is a vital link in these procedures.



In September 1973, a research project was initiated to investigate the scaling of wind tunnel store heating measurements to flight conditions. The primary objective of this project was to obtain wind tunnel and flight heating rate measurements on a pylon-mounted store to substantiate the correlation equation established from theoretical considerations. A secondary objective of this project was to investigate the influence of various store configurations (i.e., number, shape, and location) on store heating distributions. To accomplish these objectives four USAF organizations were involved in a joint effort. The organizations were:

1. Air Force Armament Laboratory (AFATL), Eglin AFB, Florida
2. Air Force Rocket Propulsion Laboratory (AFRPL), Edwards AFB, California
3. Air Force Flight Test Center (AFFTC), Edwards AFB, California
4. Arnold Engineering Development Center (AEDC), Arnold AFS, Tennessee.

The general areas of responsibility of each of the above were as follows:

<u>Organization</u>	<u>Area of Responsibility</u>
AFATL	Overall project sponsor
AFRPL	Store data recording system (flight test)
AFFTC	Flight testing (F-111 aircraft)
AEDC	Store instrumentation and wind tunnel testing plus analysis of results

The involvement of AFRPL came about from a fortunate coincidence. In the late sixties, AFRPL initiated a project to evaluate the service life of propellant grain. Their project was concerned with the Determination of Aircraft Missile Environments (Project DAME) and utilized the aft section of a Bomb Dummy Unit (BDU-12) as illustrated in Fig. 3. By 1973, an onboard data recording system had been fabricated, and twelve flights had been flown on the F-111 aircraft (Fig. 4). Since some data recording channels were available, the AFATL/AEDC store heating project was conducted as a "piggyback" effort connected with Project DAME.

The wind tunnel phase of the store heating project was conducted in the 40- by 40-in., continuous-flow tunnel of the AEDC von Kármán Facility (Tunnel A). This report documents the major results from both the wind tunnel and flight test phases of this project. In any experimental program, it is important that the test be guided by an understanding of the important parameters and more specifically by theoretical estimates. Some of the theoretical considerations that guided the present experimental program are discussed in the next Section.

## 2.0 THEORETICAL CONSIDERATIONS

Theoretical calculations of the interference flow field about a pylon-mounted store are extremely difficult, and, as previously mentioned, Epstein (Ref. 2) commented that the flow field defies analytical description. Baker, et al. (Ref. 3), presented photographs which vividly illustrated the flow-field complexity. Edney (Ref. 5) classified shock interference patterns and the associated heating amplification factors into six types. However, the specific conditions of his study could not be generalized. The discrepancies that can occur from improper use of these results were documented in Ref. 6 where it was shown that amplification factors 10 times larger than estimated were observed for a mated shuttle configuration for wind tunnel tests at Mach 8.

Conversely, the calculations of the flow field about a store in an interference-free flow field are relatively straightforward and can provide an insight as to the form of the aerodynamic scaling law. To investigate the significant parameters and to guide the experimental work, the Spalding-Chi turbulent heating method (Ref. 7) has been utilized. Calculations of the Stanton number distribution on the BDU were performed for nominal conditions corresponding to those of the wind tunnel test and for conditions corresponding to those of the flight test. A summary of the approximate conditions is:

<u>Parameter</u>	<u>Wind Tunnel</u>	<u>Flight</u>
$M_\infty$	2.0	2.0
BDU length, in.	7.90 (1/15 scale)	118.5
$Re_{\infty, L}$	$2.76 \times 10^6$	$38.6 \times 10^6$
$T_w/T_o$	0.75 to 0.96	0.60 to 0.96

The results of these calculations are presented in Fig. 5 in terms of St and  $Re_{\infty, x}$ . For these conditions the effect of wall temperature is insignificant (<5 percent) and can be neglected. The Reynolds number difference attributable to the relatively small model size (7.9 in. compared with 118.5 in. full scale) can be correlated by an equation of the form

$$St (Re_{\infty, x})^n = \text{const} \quad (1)$$

or

$$\left[ St (Re_{\infty, x})^n \right]_{wt} = \left[ St (Re_{\infty, x})^n \right]_{flt} \quad (2)$$

For turbulent boundary layers, the classical value of  $n$  is 0.2. However, by utilizing the semi-empirical Spalding-Chi solutions, it is possible to determine the value of  $n$  for the specific conditions of current interest.

Consider a given nondimensional location on the BDU (e.g.,  $x/L = 0.3$ ). For this location,

$$St_{flt} = St_{wt} \left( \frac{Re_{\infty, x_{wt}}}{Re_{\infty, x_{flt}}} \right)^n \quad (3)$$

Since the Reynolds numbers are known and the Stanton numbers can be obtained from the Spalding-Chi solutions, the only unknown in this equation is  $n$ . The "best" value of  $n$  for  $0.05 \leq x/L \leq 0.45$  was determined to be 0.17, and the correlation obtained by using this value is illustrated in Fig. 6.

It should be emphasized that the above results are based on interference-free flow-field calculations, and the actual correlation from experimental data may be somewhat different; however, the basic form should remain the same. That is,

$$St_{flt} = St_{wt} \left( \frac{Re_{\infty, x_{wt}}}{Re_{\infty, x_{flt}}} \right)^n \quad (4)$$

where  $n \approx 0.17$ .

### 3.0 DESCRIPTION OF EXPERIMENTAL PHASES

#### 3.1 WIND TUNNEL PHASE

In 1973, Matthews, et al., documented (Ref. 4) the results of wind tunnel tests on a 0.05-scale model of a store mounted on an F-4. The test technique utilized temperature sensitive thermographic phosphor paint, and produced very vivid thermal mappings of the store heating patterns. Typical photographs from this test are presented in Fig. 7. In addition to these photographs, quantitative data were also produced as shown in Fig. 8. The experimental data fairing in this figure is compared with a theoretical heating distribution based on interference-free flow-field calculations. It is common practice to compare undisturbed (interference-free) and disturbed (interference) data since reliable theoretical techniques are not available for complex flow fields. In Fig. 8, the 100-percent increase in heating at  $x/L = 0.5$  was attributed to shock impingement from a simulated fuel tank mounted on the outboard pylon. This shock impingement can be seen in the shadowgraph picture presented in Fig. 9 which was also obtained from Ref. 4.

The wind tunnel test techniques documented in Ref. 4 clearly showed that flight testing was not the only tool available to the engineer responsible for defining store thermal environments. However, this test had several major deficiencies:

1. The photographic technique of defining heating distributions (Fig. 7) was limited to those areas in camera view.
2. The uncertainty of the thermographic phosphor data ( $\pm 40$  percent) was greater than desired.
3. Existing models were utilized resulting in configurations which were unrealistic (i.e., F-4 with MK-84's and fuel tanks at  $M_\infty = 2.0$ ).

The present wind tunnel tests\* circumvented these problems by utilizing heat gages on a model of a store configuration which had previously been flight tested on the F-111 up to Mach 2.5.

The wind tunnel phase of the project was conducted in the VKF Tunnel A. Tunnel A (Fig. 10) is a continuous-flow, closed-circuit, variable density wind tunnel with an automatically driven flexible-plate-type nozzle and a 40- by 40-in. test section. The tunnel can be operated at Mach numbers from 1.5 to 6 at maximum stagnation pressures from 29 to 200 psia, respectively, and stagnation temperatures up to 750°R. Minimum operating pressures range from about one-tenth to one-twentieth of the maximum at each Mach number. The tunnel is equipped with a model injection system which allows removal of the model from the test section while the tunnel remains in operation. A description of the tunnel and airflow calibration information may be found in Ref. 9.

The parent aircraft used for this wind tunnel test program was a 1/15th-scale model of the F-111 which was provided by General Dynamics, Fort Worth. This model was originally intended for side wall mounting (i.e., a half-span model); however, for the current test it was necessary to sting mount the model and utilize the model injection system described above. To provide sting mounting and to better duplicate the F-111 flow, a model support and nose section were fabricated to simulate the right side of the fuselage. Figure 11 shows the model in the Tunnel A test section. The store mounted on the inboard pylon is a 1/15th-scale model of the BDU-12. A close-up picture of this store (Fig. 12) clearly shows the heat gages along the model axis, and an inspection of the nose region shows carborundum grit distributed around the nose. Grit is commonly used in wind tunnel testing to produce a turbulent boundary layer when the test Reynolds numbers are well below the flight values. A unique feature of the BDU models used

---

\*Some of this test work was also described in Ref. 8.

during this test was the capability to roll the model 360 deg about its axis while mounted to the pylon. This feature was incorporated in the design so that the heat gages could be rolled into any position. With this capability, data could be obtained on the inboard side of the store, thereby circumventing the shortcoming of the photographic test technique previously used (see Fig. 7).

In addition to the BDU model shown in Fig. 12, three other store models were fabricated:

1. Second BDU heat gage model,
2. BDU pressure model, and
3. GBU-8 heat gage model.

A photograph of the two heat gage models mounted on the F-111 is presented in Fig. 13. Because of its fin geometry, the GBU-8 model was limited to the discrete roll positions of 0 and 180 deg. However, heat gages were installed at three circumferential positions ( $\phi_{INST} = 22.5, 90, \text{ and } 157.5 \text{ deg}$ ); thus, by rolling the model 180 deg, the gages were positioned at three more locations ( $\phi_{INST} = 202.5, 270, 337.5 \text{ deg}$ ).

By utilizing the store roll capability just described and by interchanging the store mounting position, a large amount of store interference data was obtained. The specific configurations tested are illustrated in Fig. 14.

The test was conducted at Mach numbers of 1.75, 2.0, and 2.5. The free-stream unit Reynolds number ranged from 1.4 million to 5.2 million per foot. A summary of the specific test conditions for each configuration is presented in Table 1.

The tunnel stilling chamber conditions and the BDU pressure data were measured with the standard Tunnel A pressure system which is described in Ref. 9. The heat-transfer data were obtained with gages designed, fabricated, and calibrated at AEDC.

During a typical heat-transfer run, the model was injected into the airstream at a relatively cool initial temperature and held at a fixed position while the store was heated. Each gage measured both a heating rate ( $\dot{q}$ ) and a "wall" temperature ( $T_w$ ) during the heating cycle. An example illustrating the repeatability of these basic measurements is presented in Fig. 15. To convert these measurements from heating rate ( $\dot{q}$ ) to heat transfer coefficient ( $h$ ), the definition of heat-transfer coefficient was used as illustrated below:

$$h \equiv \frac{\dot{q}}{T_r - T_w} \quad (5)$$

or rearranging,

$$\dot{q} = hT_r - hT_w \quad (6)$$

But, since  $h$  and  $T_r$  are approximately constant for a given gage, we have an equation of the form

$$\dot{q} = A_o + A_1 T_w \quad (7)$$

where

$$A_o \equiv hT_r \text{ and } A_1 \equiv -h \quad (8)$$

Therefore, the slope of the data presented in Fig. 15 is identical to the negative of the heat-transfer coefficient. This same technique was used in the analysis of the flight test data.

### 3.2 FLIGHT TEST PHASE

In September 1973, initial plans for the flight test phase of the AEDC/AFATL store heating project were formulated. The test article was the BDU-12 which is a simulated nuclear ordnance. Since this specific shape had been cleared for flight to the limits of the aircraft's capability (Fig. 1) it was selected for project DAME. A photograph of the BDU nose section (Fig. 16) illustrates the location of the heat gages and additional instrumentation details are presented in Fig. 17. The primary instrumentation consisted of thermopile Gardon gages located 105 deg from the pylon on the outboard side at 13 model stations; however, only 10 stations were utilized to record data because of data channel limitations. Each Gardon gage measured both the heating rate ( $\dot{q}$  Btu/ft<sup>2</sup>-sec) and the gage wall temperature. A detailed description of these gages is presented in Ref. 10. Secondary instrumentation consisted of coaxial surface thermocouples (also described in Ref. 10) and "backside thermocouples" to measure the temperature differential across the skin of the BDU. These measurements were limited primarily to flight 14, and the results showed only slight temperature differentials. After flight 14, the hook-up was changed so that the channels with less "noise" were utilized for  $\dot{q}$  measurements (primary data) as will be discussed later.

Also installed in the BDU was a pressure package for measuring the differential pressure in the pitch and yaw planes at  $x/L = 0.05$ .

The original data acquisition system was designed and developed by the Naval Weapons Center (NWC), and a complete description of this system may be found in Refs. 11 and 12. In general, the instrumentation output signals are connected to a pulse amplitude modulation (PAM) system and are recorded on magnetic tape. The tape system is mounted inside the BDU and controlled by a hardwired on/off switch on the co-pilot's side of the cockpit. There are approximately 12 min of record time available which means that the recorder was turned on only at discrete intervals during the flights.

The aircraft used to support project DAME was one of two F-111's at the Edwards Flight Test Center (FTC). The specific aircraft was an FB-111A with tail number 70159.

Flights 1 through 12 were flown prior to AEDC involvement with project DAME, and some rocket propellant data from these flights may be found in Ref. 13. The dates and test conditions for all the flights are presented below:

<u>Flight No.</u>	<u>Dates</u>	<u>M<sub>∞</sub></u>	<u>Remarks</u>
1-12	Prior to Sept. 1973		No AEDC involvement
13	Sept. 25, 1973	2.5	Phase change paint only
14	July 18, 1974	2.0	Full VKF instrumentation
15	Aug. 22, 1974	0.85	Subsonic flight
16	April 22, 1975	2.0	Present data
17	July 16, 1975	1.67	Abort due to engine problems
18	July 26, 1975	2.0	Present data
19	July 29, 1975	2.0	Present data
20	Aug. 4, 1975	2.0	Present data

In general, an attempt was made to duplicate the conditions for each flight so that the data quality could be determined in part by its repeatability. The desired nominal test conditions were: Mach 2 at 40,000 ft with  $\alpha = 4$  deg. This was achieved on flights 14, 16, 18, 19, and 20. Flight 15 was a subsonic mission to perform afterburner tests, and flight 17 was aborted at Mach 1.67 because of an engine failure. The specific test conditions in terms of static temperature, altitude, Mach number, and angle of attack are presented in Fig. 18, and additional details of this flight test program were published in Ref. 14.

## 4.0 RESULTS AND DISCUSSION

### 4.1 WIND TUNNEL PHASE

As noted in the test summary (Table 1), a very large volume of data was obtained during these tests. In this section, selected results will be presented which pertain to the secondary objective of investigating the influence of various store configurations on store heating distributions. The correlation of wind tunnel and flight test data which was the primary objective will be presented in Section 4.3.

Before presenting the interference heating data, it is important to establish reference heating distributions. The reference level normally used is an undisturbed or interference-free value and can be based on theoretical calculations or experimental measurements. In the present case, experimental measurements were used. An illustration of the  $\alpha = 0$ , "undisturbed" data used for the BDU is presented in Fig. 19. These data were obtained with the same model that was used for the "disturbed" data obtained with the model mounted in the interference flow field of the F-111. For  $x/L > 0.3$ , the data fairing shows good agreement with turbulent theoretical calculations based on the method of Spalding and Chi. For  $x/L < 0.3$ , the data exhibited the "classical overshoot" of a transitional boundary layer. This figure demonstrates that the grit affixed to the BDU nose (see Fig. 12) was indeed effective in producing a turbulent boundary layer on this relatively small model (1/15th scale). In addition to substantiating that the grit produced a turbulent boundary layer, Fig. 19 also indicates the data repeatability (generally  $\pm 10$  percent).

It is also important to note that the data and theory of Fig. 19 are for an angle of attack of 0 deg while the majority of the data in this report will correspond to 4-deg angle of attack. This was done to simplify the theoretical computations\* and to provide a single reference value for the interference data at any angle of attack. Similar undisturbed reference data were also obtained for the GBU model.

Interference heating distributions measured on the BDU at a radial position of 105 deg\*\* from the pylon are presented in Fig. 20. The data fairings are for two Reynolds numbers and an angle of attack of 4 deg. This angle corresponds to the nominal angle of attack of the Mach 2 portion of the flight test. The data are relatively insensitive to angle of attack while increasing the free-stream Reynolds number from  $1.86 \times 10^6$  to  $2.76 \times 10^6$  produces a slight ( $\approx 20$  percent) increase in heating level. Based on these data and on the uncertainties in the gage calibration factors, the estimated precision of the wind

---

\*Theoretical calculations for  $\alpha \neq 0$  are more complex and are less precise.

\*\*Note that this location and configuration are identical to those of the flight test.



tunnel data is  $\pm 10$  percent. The high Reynolds number,  $\alpha = 4$  deg data presented in Fig. 20 will be used in the wind tunnel/flight correlation in Section 4.3. The increase (or decrease) in heating caused by the interference generated by the parent aircraft and the pylon can be quantified by the use of "amplification factors." These amplification factors are simply the ratio of the heating from the F-111 pylon-mounted stores to those of the undisturbed case at a given model location. That is;

$$AF \equiv h/h_u = \left( \frac{\text{heating measured with pylon mounting}}{\text{heating measured in undisturbed flow}} \right)_{\text{each gage}} \quad (9)$$

Typical data showing the level and circumferential distribution of the amplification factors ( $h/h_u$ ) for the various configurations tested are presented in Fig. 21. The solid symbols in Fig. 21 illustrate the data repeatability. It is important to notice that almost all the amplification factors are below 1.5 and that a large percentage is below 1.0. This statement is true for all the data obtained during this test and is not limited to the relatively small sample presented in this report. It has been shown (Ref. 5) that for some conditions interfering flow fields can produce large amplification factors. The present data show that the interference heating at  $\alpha = 4$  deg was within  $\pm 50$  percent of that for an undisturbed flow field at zero angle of attack. Therefore, within the scope of the present investigation, preliminary engineering estimates of store thermal environments can be based on undisturbed flow-field calculations. It should be noted that no particular effort was made to locate or resolve regions of high heating, and some small regions of large interference may have been missed. Therefore, general application of the preceding conclusion should be avoided until further verification is made via a concerted effort to locate and resolve the magnitude of localized hot spots.

Circumferential pressure distributions for Configuration 1 (see Fig. 14) are presented in Fig. 22. This was the only configuration on which pressure measurements were obtained. The number of instrumented locations was limited\* because of the relatively larger size of pressure tubing as compared with the electrical wires for the heat gages. Figure 22 also shows theoretical levels based on the method of characteristics for an undisturbed flow field. It is interesting to note that the experimental pressure data at  $x/L = 0.15$  are above the theoretical value (1.14), while at  $x/L = 0.35$ , the experimental data are below the undisturbed value (0.92).

---

\*This 1/15th-scale pressure model had a total of eight tubes installed as opposed to 26 heat gages in the same size heat model.

In Ref. 15, Van Aken and Markarian used pressure data to predict heating distributions by applying a correlation equation of the form:

$$h/h_u = \left[ \frac{(p/p_\infty)}{(p/p_\infty)_u} \right]^{0.85} \quad (10)$$

The pressure distributions presented in Fig. 22 were substituted into this equation to give the interference heating predictions shown in Fig. 23. These predicted heating distributions are compared with the present experimental heat transfer measurements and, in general, the data correlation was within 20 percent.

## 4.2 FLIGHT TEST PHASE

The first flight in which AFATL/AEDC was involved occurred in September 1973 (Flight 13). This particular flight utilized an F-model of the F-111 and was capable of supersonic carriage of the BDU-12 at a Mach number of 2.5. Of course, this store did not contain TNT and was in no way restricted by the temperature limitations previously discussed. This Mach 2.5 flight clearly demonstrated that present-day aircraft do have the required thrust for supersonic carriage of large stores. Figure 24 shows a photograph of the store just prior to the flight. The circumferential stripes on the front half of the BDU are Tempilaq<sup>®</sup> paint. Tempilaq paint changes phase from a solid to a liquid (melts) at a specific temperature. The paints consist of calibrated melting point materials suspended in an inert carrier. The paint melting point temperatures used for Flight 13 were 300, 250, 200, and 150°F. The postflight photograph presented in Fig. 25 vividly shows the flow patterns produced by the pylon shock and by the sway-brace hardware. These patterns correspond to local streamlines and are produced as the paint melts and the local shear forces cause the melted paint to flow. Of course, the paint doesn't melt until the local wall temperature reaches the specific melt temperature of the paint (e.g. 150°F). These paints are commonly used in wind tunnel testing, and this flow visualization technique is a good example of the application of wind tunnel techniques to flight testing. However, it should be mentioned that the second and only other attempt to use this technique did not produce photographs of the quality shown in Fig. 25.

The flight test parameters shown in Fig. 18 were determined directly from the aircraft instrument panel. In addition to the aircraft instrumentation, a weather balloon was sent aloft. Unfortunately, the time and location of the test flight were generally different from the balloon, and therefore, the instrument panel readings were used as the primary data for determination of the flight conditions.

Since the aircraft altimeter is set at a sea-level pressure of 29.92 in. Hg, all altitudes are based on standard-day pressure altitude. Data of interest were obtained at a pressure altitude of 40,000 ft, and using the 1962 Standard Atmosphere this gives

$$\frac{p_{\infty}}{p_o} = 0.185769 \quad \text{and} \quad p_o = 2116.22 \text{ lb/ft}^2 \quad (11)$$

$$p_{\infty} = 393.13 \text{ lb/ft}^2 = 2.73 \text{ psi} \quad (12)$$

The density at altitude was calculated as follows:

free air temperature = -74.2°F (385.8°R) (obtained from instrument panel)

$$\rho_{\infty} = 2.7 \frac{2.73 \text{ psi}}{385.8^{\circ}\text{R}} = 0.0191 \text{ lbm/ft}^3 \quad (13)$$

The viscosity for this temperature (-74°F) can be calculated from Sutherland's law, and the result is

$$\mu_{\infty} = 9.49 \times 10^{-6} \text{ lbm/ft-sec} \quad (14)$$

Substitution into the Reynolds number equation gives

$$\begin{aligned} \text{Re}_{\infty} &= \frac{\rho_{\infty} v_{\infty}}{\mu_{\infty}} = \frac{\rho_{\infty} M_{\infty} a_{\infty}}{\mu_{\infty}} = \frac{\rho_{\infty} M_{\infty} 49.02 \sqrt{T_{\infty}}}{\mu_{\infty}} \\ &= \frac{(0.0191) (2.02) (49.02) \sqrt{385.8}}{9.49 \times 10^{-6}} \end{aligned} \quad (15)$$

$$\text{Re}_{\infty} = 3.91 \times 10^6 \text{ ft}^{-1} \quad (16)$$

which is the nominal flight Reynolds number.

A comparison of initial zeros and final zeros for Flights 16 and 18 is presented in Fig. 26. In this figure and in subsequent figures, the symbols represent the average of 150 readings. The elapsed time interval for these 150 readings is only 10 sec, and the aircraft is parked; therefore, these readings should be identical for a "noise" free system. The bar symbol (I) represents the maximum and minimum values obtained in the data readings. The source of the "noise" illustrated in Fig. 26 is believed to be attributable to the recording system.

An illustration of the relative "noise level" for each flight is presented in Fig. 27. The deviation shown corresponds to that of channel 54 during the Mach 2 portion of each flight. It should be emphasised that this figure shows "noise level" and not data

precision. It is also important to note that Flight 14 exhibited a lower "noise level" than any of the other flights.

Data from Flight 14 are presented in Fig. 28 in terms of the measured gage parameters  $\dot{q}$  and  $T_w$ . This figure illustrates the technique used to reduce the basic measurements to a heat-transfer coefficient ( $h$ ). This data reduction technique was recently developed for the VKF supersonic Tunnel A as was previously discussed and it has proved to be particularly useful when the driving potential ( $T_r - T_w$ ) is relatively small as was the case for the present flights.

From the plot  $\dot{q}$  vs  $T_w$ , the data should be a straight line with a slope equal to  $-h$  as illustrated in Fig. 28. As previously mentioned, each symbol corresponds to the average of 150 data recordings, and this particular set of data is from Flight 14 which was the flight with the lowest "noise level." As can be seen even for the "best" case, all the data points do not fall on the straight line. In a large percentage of the cases, it was not possible to determine a value of heat-transfer coefficient ( $h$ ) because of the scatter in the data. A complete presentation of all the  $h$  values determined is given in Fig. 29, and as expected, there is a general lack of repeatability, particularly with regard to Flight 14 (circle symbol). The values of inferred recovery temperature ratio (i.e.,  $T_r/T_o$ ) was 0.94 for Flight 14, while the remaining flights produced a nominal value of 0.89. A theoretical value of 0.96 was predicted. The temperature rise of the BDU wall which occurred during the acceleration to Mach 2 is presented in Fig. 30. Also shown are the ambient air temperature and the calculated recovery temperature ( $T_r$ ). The main conclusion from these data is that the BDU temperatures reached or exceeded 178°F during the 4 min of sustained Mach 2 flight.

### 4.3 CORRELATION OF WIND TUNNEL AND FLIGHT TEST DATA

The need for defining the thermal environment of externally carried weapons is apparent since they contain explosives, sensors, fuzes, and electronic components which can malfunction at elevated temperatures (165°F or higher). As shown in Section 4.2, temperatures in excess of 165°F are easily obtainable with today's high-performance aircraft, particularly when operating in "hot" climates. To determine if critical components buried within the weapon actually exceed their thermal specifications requires a sophisticated thermal analysis. However, this analysis is only as good as the basic input information. The two most important input parameters for a thermal analysis are recovery temperature ( $T_r$ ) and heat transfer coefficient ( $h$ ).

Recovery temperature ( $T_r$ ) can be estimated by the simple equation:

$$T_r = T_e (1 + 0.18 M_e^2) \quad (17)$$

where  $T_e$  and  $M_e$  are the boundary-layer edge temperature and Mach number, respectively. For most locations (excluding the nose region) a first approximation is  $T_e \approx T_\infty$  and  $M_e \approx M_\infty$ , where  $T_\infty$  is the ambient air temperature and  $M_\infty$  is the free-stream Mach number. A plot of the above equation for various free-stream temperatures and Mach numbers is presented in Fig. 31. Also shown in Fig. 31 is a nominal limiting component temperature level of 165°F. Note that if the ambient temperature is -70°F, operations up to Mach 1.8 are possible without overheating the store. On the other extreme, if the ambient temperature is 130°F, limited flight times are required for all Mach numbers above 0.6. The intent of this figure is to illustrate that ambient air temperature (as well as aerodynamic heating) is an extremely important parameter in the analysis of store thermal environments.

If conditions are such that flight time must be limited to avoid overheating critical components, the important parameter is heat-transfer coefficient. To determine the allowable flight time, the heat-transfer distribution is used as the input to a computer code which computes heat conduction from the surface to the internal components (see Ref. 15, for example).

The most cost-effective way to obtain heat-transfer distributions for flight conditions is the extrapolation of wind tunnel measurements. As previously discussed, one of the primary objectives of the current program was the substantiation of the extrapolation procedures which were derived in Section 2.0. The significance of this is further illustrated in Fig. 32, which compares the wind tunnel and flight test Reynolds numbers. The size of the BDU model was only 7.9 in. compared with 118.5 in. for the actual flight hardware. The ability to obtain heating distributions on this small model and then to use these measurements to infer the heating distributions for the actual flight hardware is an important link in defining thermal environments. The substantiation of this link requires specific comparison of wind tunnel and flight test data. The flight test data on the BDU mounted on the F-111 were presented in Fig. 29, and the corresponding\* wind tunnel data were presented in Fig. 20. Figure 33 shows these same data presented in terms of the correlation parameter  $St(Re_{\infty,x})^{0.17}$ . Unfortunately, the scatter of the flight test data prohibits any definite conclusion regarding the substantiation of this correlation parameter. However, it is interesting to note that the flight data which show best agreement with the wind tunnel data are the data from Flight 14 which were considered

---

\*Same  $M_\infty$ , same  $\alpha$ , same configuration.

to be the most reliable of the flight results. Therefore, there is some evidence to substantiate the correlation parameter  $St(Re_{\infty,x})^{0.17}$ ; however, better quality flight data are needed.

Based on the experience gained during this project a new stand-alone airborne data recording system is currently being developed. This system, shown in Fig. 34, will be operational in October 1978 and will be capable of recording 112 data channels for a period of up to 40 min. Additional details describing this system may be found in Ref. 16.

## 5.0 CONCLUSIONS

Flight and wind tunnel heat-transfer measurements have been made on a pylon-mounted store on an F-111. The flight test data were obtained during constant altitude (40,000 ft) and constant Mach number ( $\approx 2.0$ ) flights at Edwards AFB. The 1/15-scale wind tunnel tests were conducted in the 40- by 40-in. Tunnel A at the AEDC. The purpose of these tests was to substantiate wind tunnel-to-flight extrapolation procedures, and to investigate the effects of various store configurations on store heating distributions. Some of the major conclusions from this work are listed below.

### Wind Tunnel Tests

1. The wind tunnel tests have demonstrated the versatility of scale model testing and the application of testing techniques to define store pressure and heat-transfer distributions.
2. Within the scope of the present experiment, the measured heating amplification factors were less than 1.5 which means, that for preliminary estimates, store thermal environments can be based on undisturbed flow field calculations. However, it should be recognized that small localized "hot spots" may exist and should be considered in the final analysis.
3. The pressure and heat-transfer data were correlated within 20 percent by the equation used by Van Aken and Markarian (Ref. 15).

### Flight Test

1. The application of wind tunnel technology to the aircraft/store compatibility field has been demonstrated (e.g., phase-change paint, gage data reduction, etc.).

2. The BDU inside case temperatures reached or exceeded the temperature at which TNT melts (178°F) within 4 min of sustained Mach 2 flight.

### Flight and Wind Tunnel Comparisons

1. Ambient air temperature was shown to be a very important parameter in the analysis of store thermal environments.
2. Scatter in the flight-test data prohibited any definite conclusion regarding the substantiation of the correlation equation.
3. Based on the experience gained during these tests a new stand-alone airborne data recording system is being fabricated.

### REFERENCES

1. Budemholzer, R. A., Goldsmith, A., and Nielsen, H. J. "Investigation of Problems of Temperature and Pressure Influencing the Design of Bomb Weapons." AFAC-TR-57-112(I), November 1957.
2. Epstein, Charles S. "Supersonic Delivery of Conventional Weapons - Fact or Fancy?" Aircraft/Stores Compatibility Symposium, AFFDL-TR-72-67, Vol 1, pp. 51-72, August 1972.
3. Baker, S. S. and Matthews, R. K. "Demonstration of the Thermographic Phosphor Heat-Transfer Technique as Applied to Aerodynamic Heating of External Stores." AEDC-TR-73-128 (AFATL-TR-73-154)(AD769306), August 1973.
4. Matthews, R. K., Baker, S. S., and Capt. Key, J. C., Jr. "Wind Tunnel Heating Test of Aircraft Stores." Aircraft/Stores Compatibility Symposium Proceedings, JTCG/ALNNO WP-12-2, Vol. 4, September 1973.
5. Edney, Barry E. "Shock Interference Heating and the Space Shuttle." NASA TMX-52876. Vol. I, July 1970.
6. Matthews, R. K., Eaves, R. H., Jr., and Martindale, W. R. "Heat-Transfer and Flow-Field Tests of the McDonnell Douglas-Martin Marietta Space Shuttle Configurations." AEDC-TR-73-53 (AD759176), April 1973.
7. Spalding, D. B. and Chi, S. W. "The Drag of a Compressible Turbulent Boundary Layer on a Smooth Flat Plate with and without Heat Transfer." Journal of Fluid Mechanics, Vol. 18, 1964.

8. Matthews, R. K., Spencer, George D., and Key, James C., Jr. "Pressure and Heat-Transfer Measurements on Several Pylon-Mounted Store Configurations." Aircraft/Store Compatibility Symposium, JTCG/MD, Fort Walton Beach, Florida, October 1977.
9. Test Facilities Handbook (Tenth Edition). "von Kármán Gas Dynamics Facility, Vol. 4." Arnold Engineering Development Center, May 1974.
10. Trimmer, L. L., Matthews, R. K., and Buchanan, T. D. "Measurement of Aerodynamic Heat Rates at the AEDC von Kármán Facility." International Congress on Instrumentation in Aerospace Simulation Facilities, IEEE Publication CHO 784-9 AES, September 1973.
11. Mercado, P. "Data Acquisition and Recording System for Project DAME: Part 1 System Description." Naval Weapons Center, TN304-279 Part 1, September 1972.
12. Mercado, P. "Data Acquisition and Recording System for Project DAME; Part 2 Ground Checkout and Calibration Procedures." Naval Weapons Center, TN304-279 Part 2, September 1972.
13. Jones, W. B., Jr. and Meyer, Lee. "Definition of Captive Flight Loads for Solid Propellant Grain Service Life Predictions." Paper presented at AIAA/SAE/JANNAF Propulsion Meeting, San Diego, California, October 1974.
14. Matthews, R. K. and Key, J. C., Jr. "Flight Test Heat-Transfer Measurements on a Pylon-Mounted Store." Aircraft/Stores Compatibility Symposium Proceedings, JTCG/MD WP-12, Vol. 2, September 1975.
15. Van Aken, Ray W. and Markarian, C. F. "Thermal Considerations of Stores in Captive Flight." Aircraft/Stores Compatibility Symposium Proceedings, JTCG/ALMNO WP-12-2, Vol. 4, September 1973.
16. Matthews, R. K., Tolley, H. D., and Nutt, K. W. "A Stand-Alone Airborne Data Recording System." Paper presented at 1978 Air Data Systems Conference, USAF Academy, May 1978.



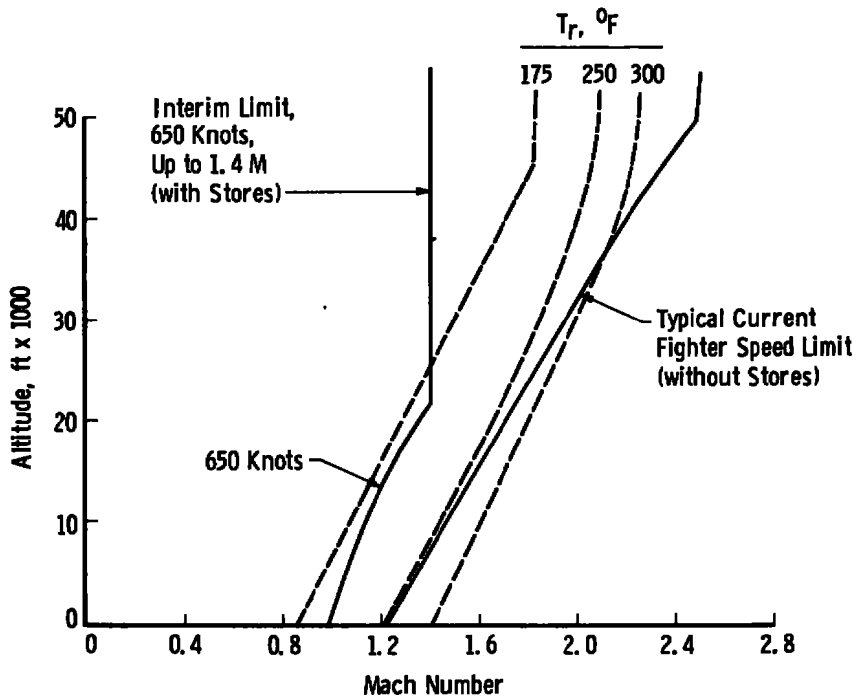


Figure 1. Performance envelope of present-day aircraft.

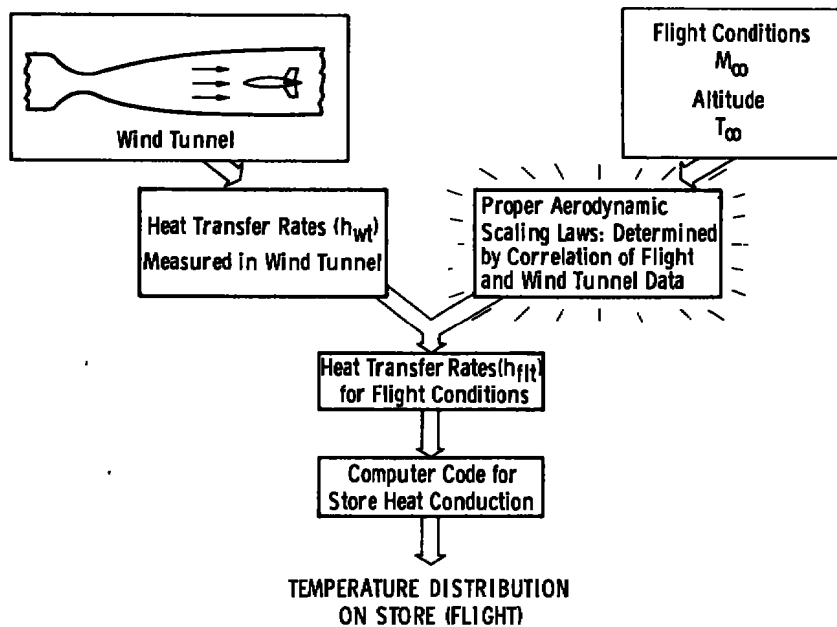


Figure 2. Schematic showing extrapolation of wind tunnel data to flight conditions.

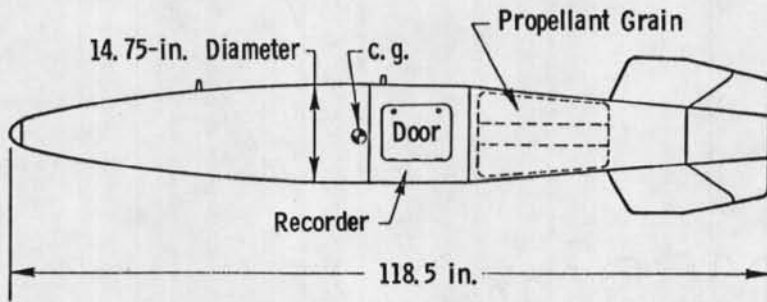


Figure 3. AFRPL project DAME test vehicle.

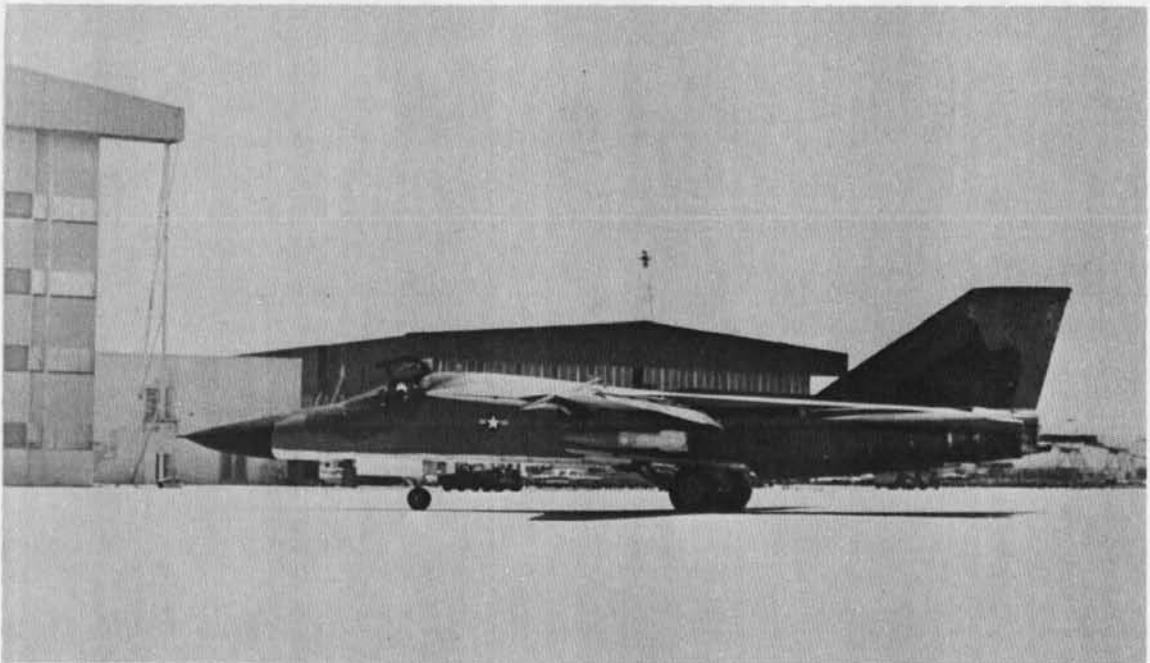


Figure 4. Photograph of pylon-mounted store on F-111.

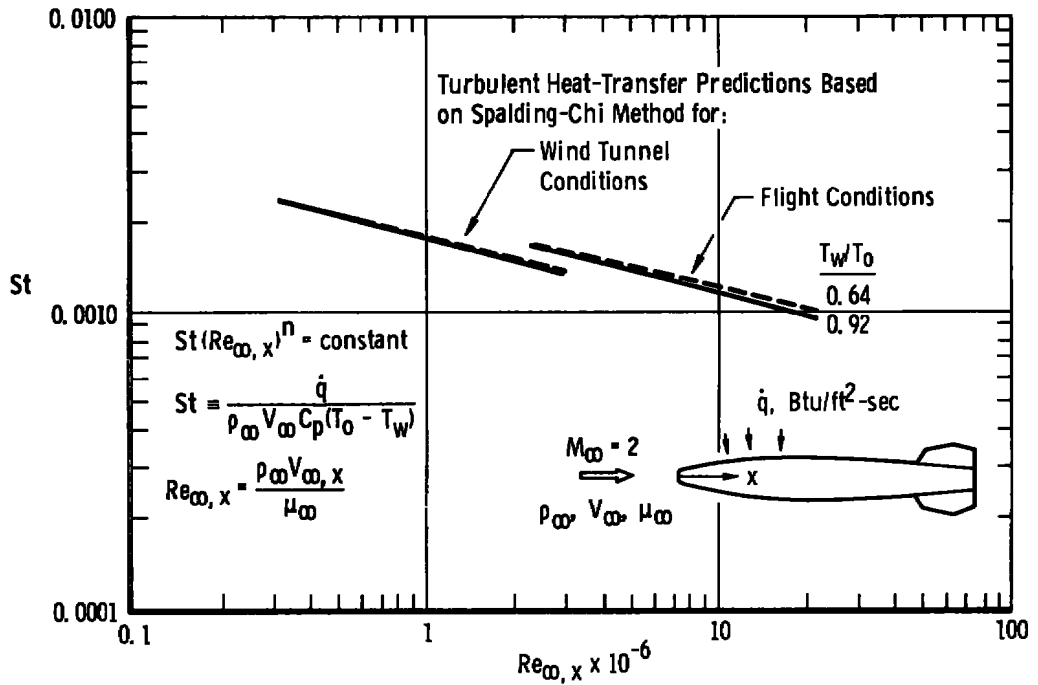


Figure 5. Effect of wall temperature and Reynolds number on store heating rates.

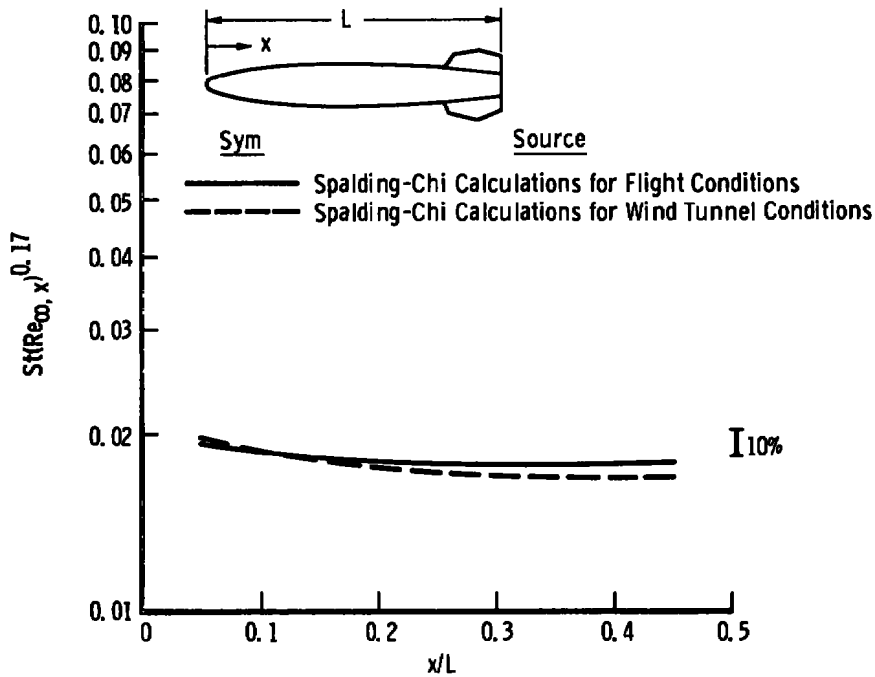
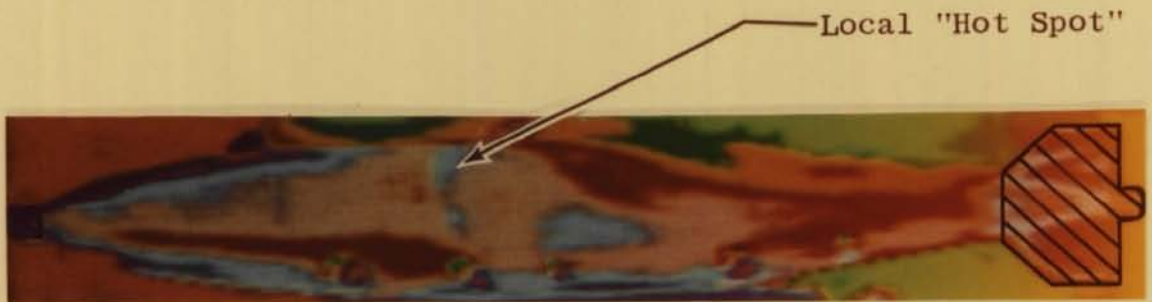


Figure 6. Illustration of extrapolation of wind tunnel predictions to flight conditions.

Increasing Value of  $h_{wt}$



Fuel Tanks Off



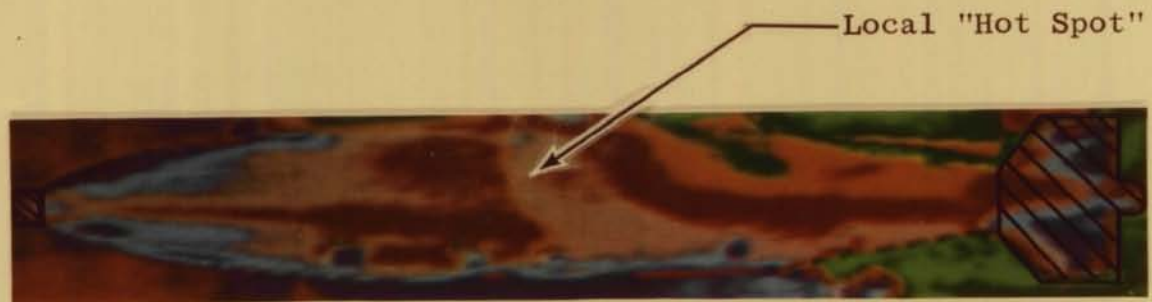
Fuel Tanks On

Crosshatching Denotes Areas of Invalid Data

a.  $M_\infty = 1.76, Re_\infty = 3.84 \times 10^6 \text{ x ft}^{-1}$



Fuel Tanks Off



Fuel Tanks On

b.  $M_\infty = 2.00, Re_\infty = 4.29 \times 10^6 \text{ ft}^{-1}$

Figure 7. Examples of heating data obtained by thermal mapping techniques (from Ref. 4).

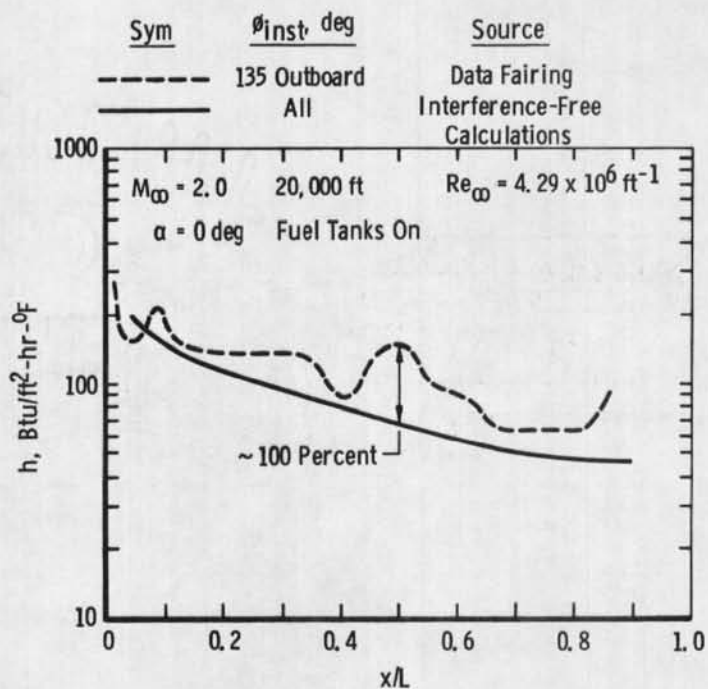


Figure 8. Comparison of data fairing with interference-free calculations (from Ref. 4).



Figure 9. Shadowgraph illustrating shock impingement (from Ref. 4).

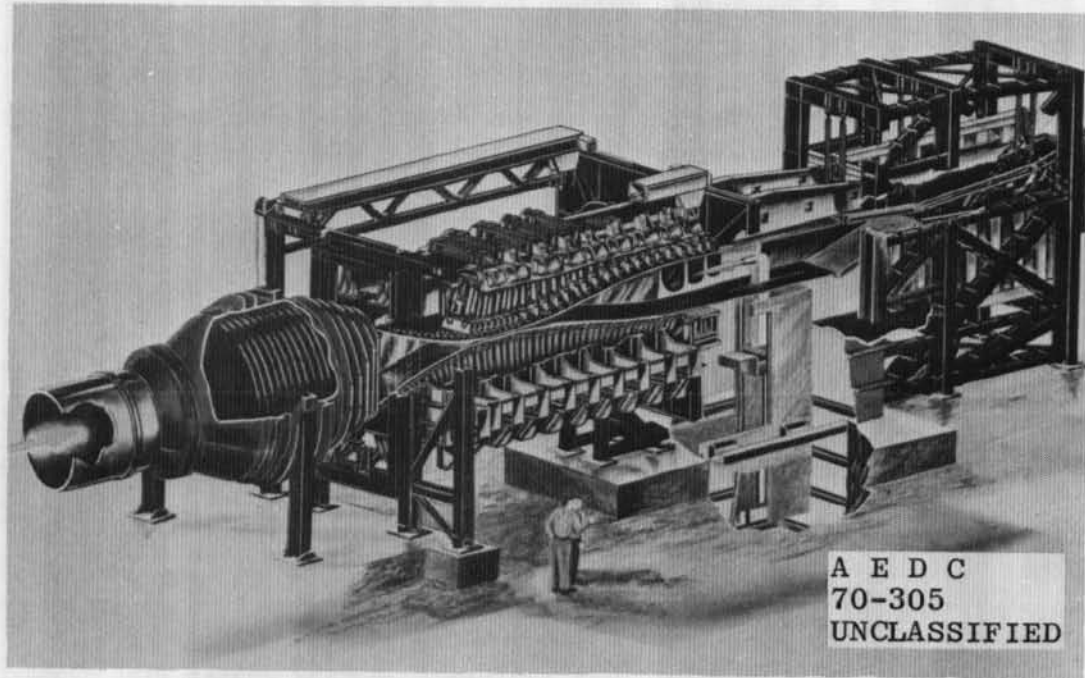
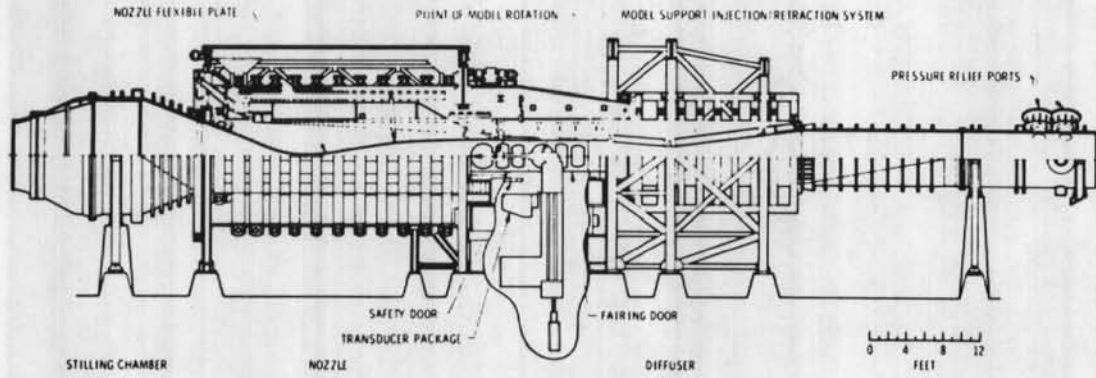


Figure 10. Tunnel A assembly.



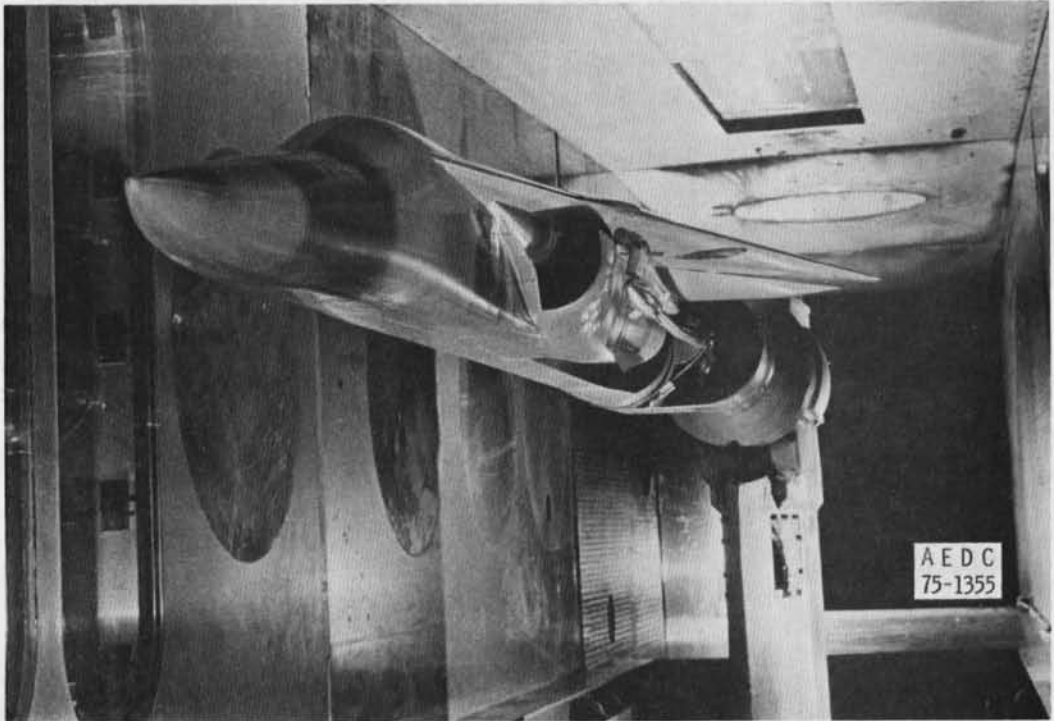


Figure 11. Photograph of 1/15th-scale model of F-111 and BDU-12 in Tunnel A test section.

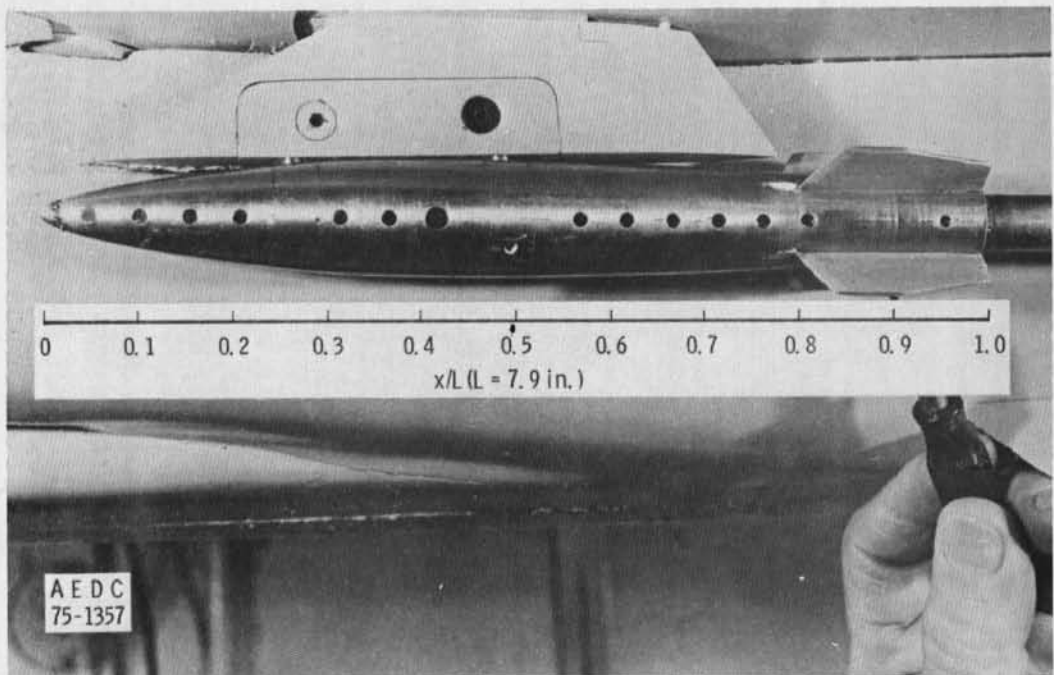
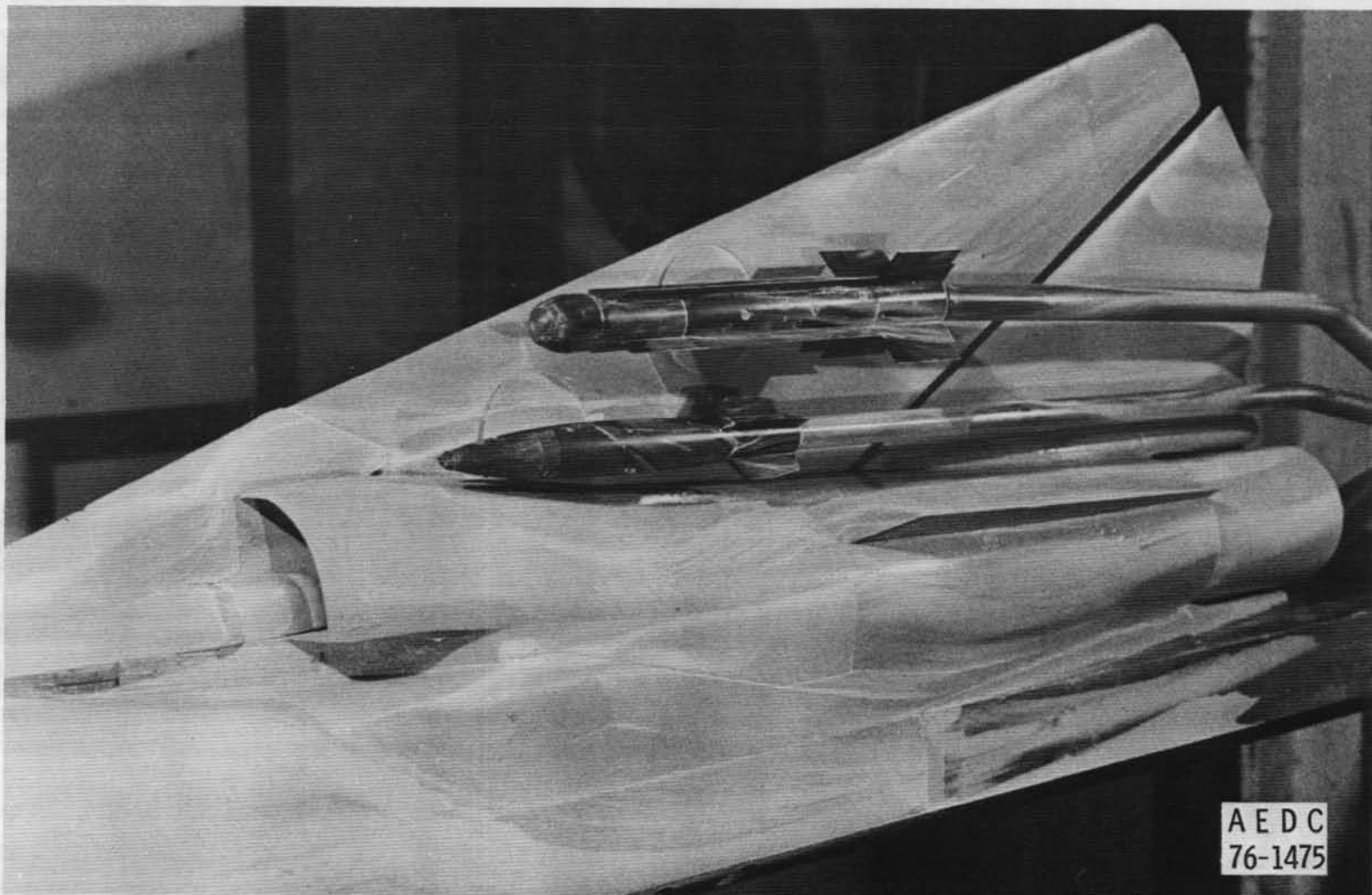
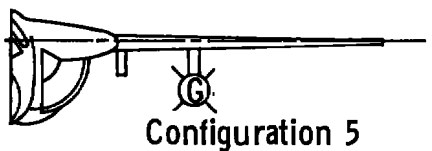
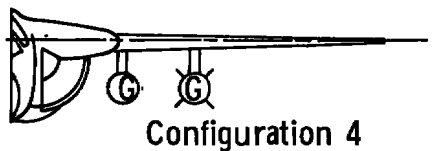
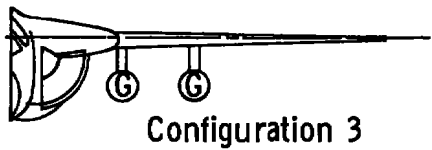
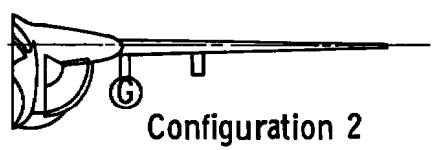
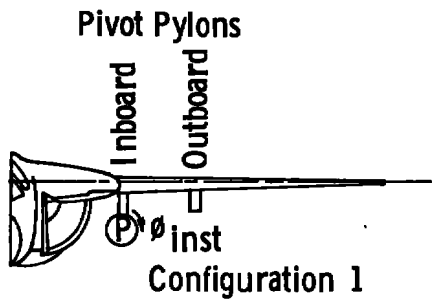


Figure 12. Photograph of heat gage BDU model.



**Figure 13. Photograph of GBU (outboard) and BDU (inboard) in carriage position on F-111 model.**





LEGEND

- Ⓟ BDU Pressure Model
- Ⓞ BDU Heat Gage Model
- Ⓧ BDU Heat Gage Model

Note: Intereference-free data were also obtained on all store models (i.e., Store Alone, no F-111).

1/15-th Scale Model

Figure 14. Configurations tested in Tunnel A.

Undisturbed BDU Data

$x/L = 0.65$

Sym	Run No.
*	1
+	2
x	5

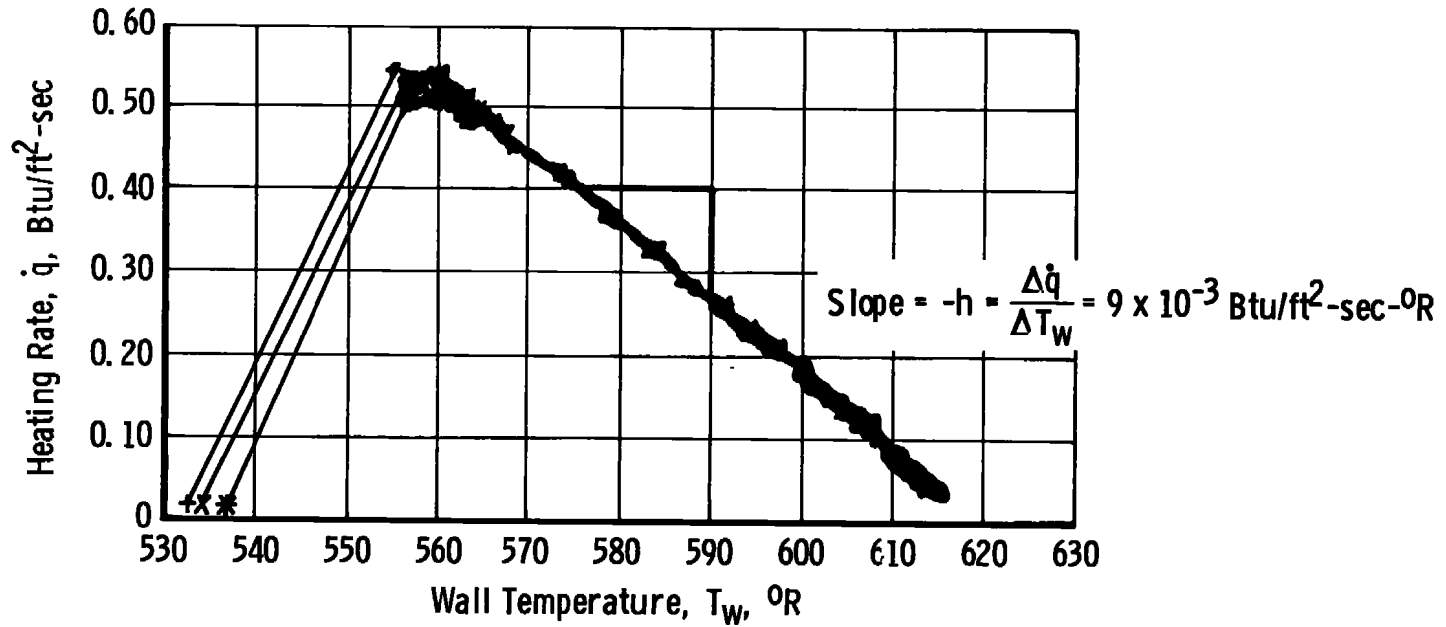


Figure 15. Illustration of heat gage data reduction technique (wind tunnel).

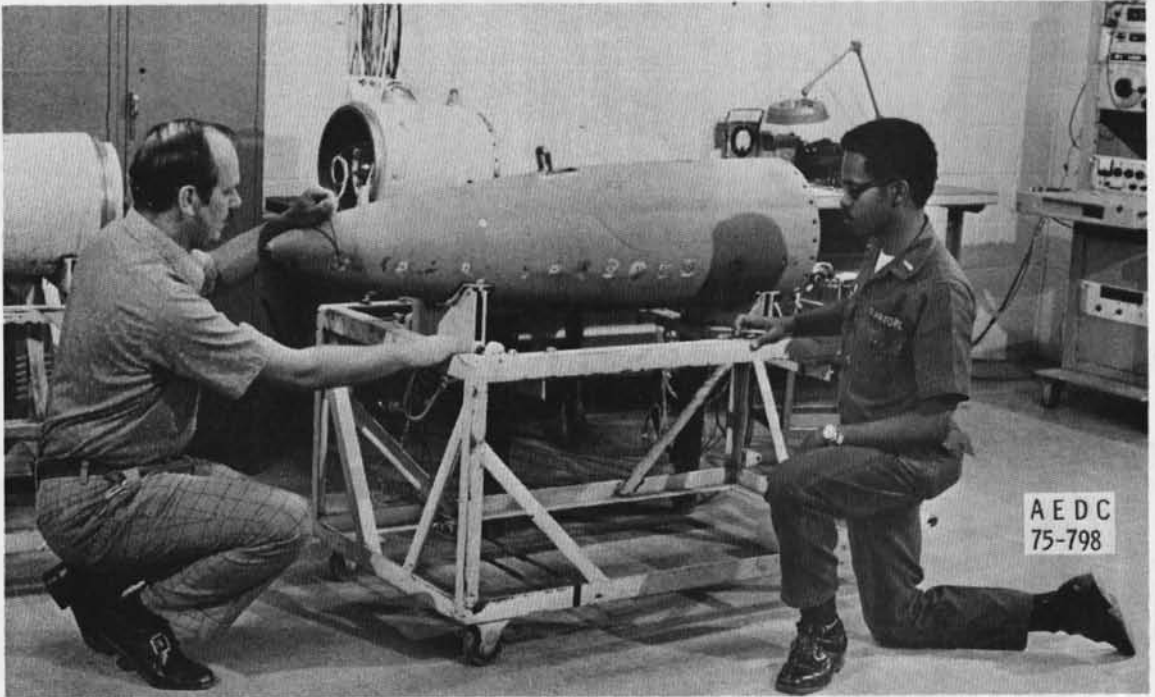


Figure 16. Photograph of BDU nose with VKF gages installed.

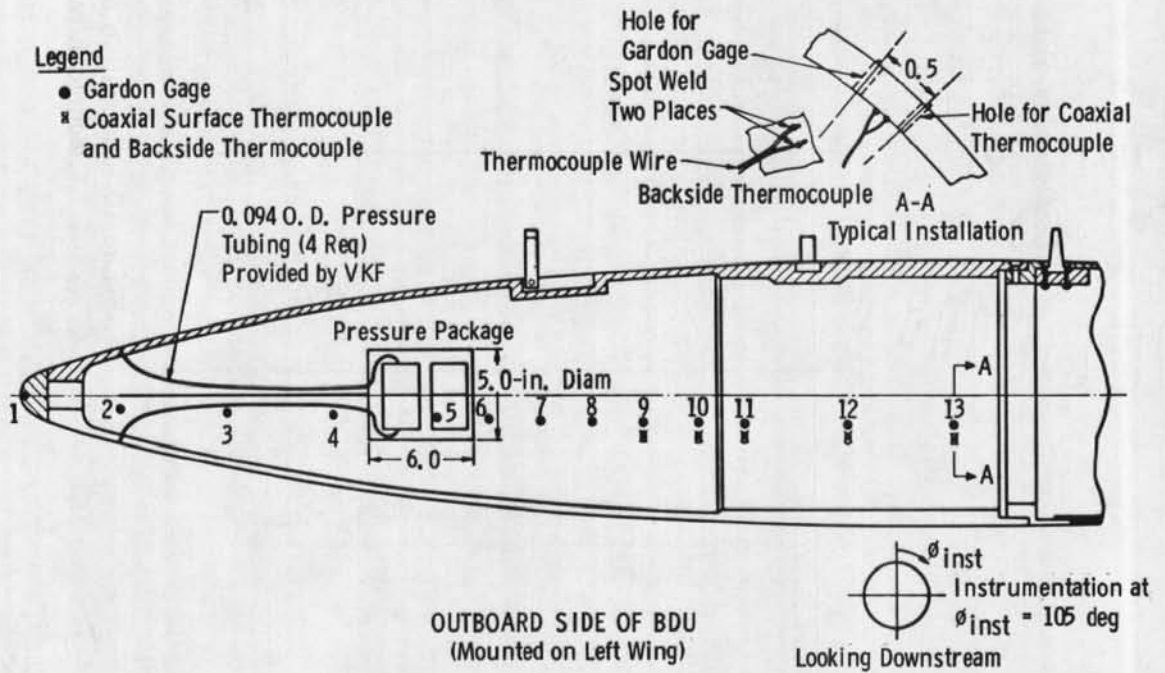


Figure 17. VKF instrumentation for BDU aerodynamic heating test at Edwards AFB.

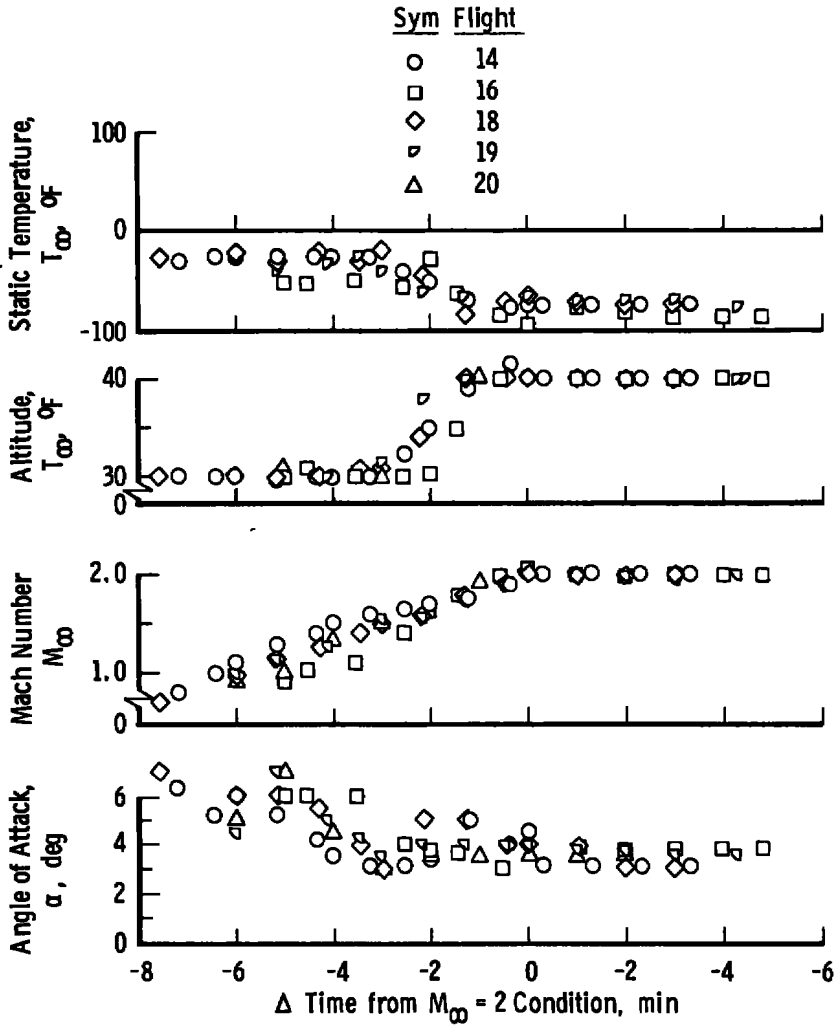


Figure 18. Flight test conditions.

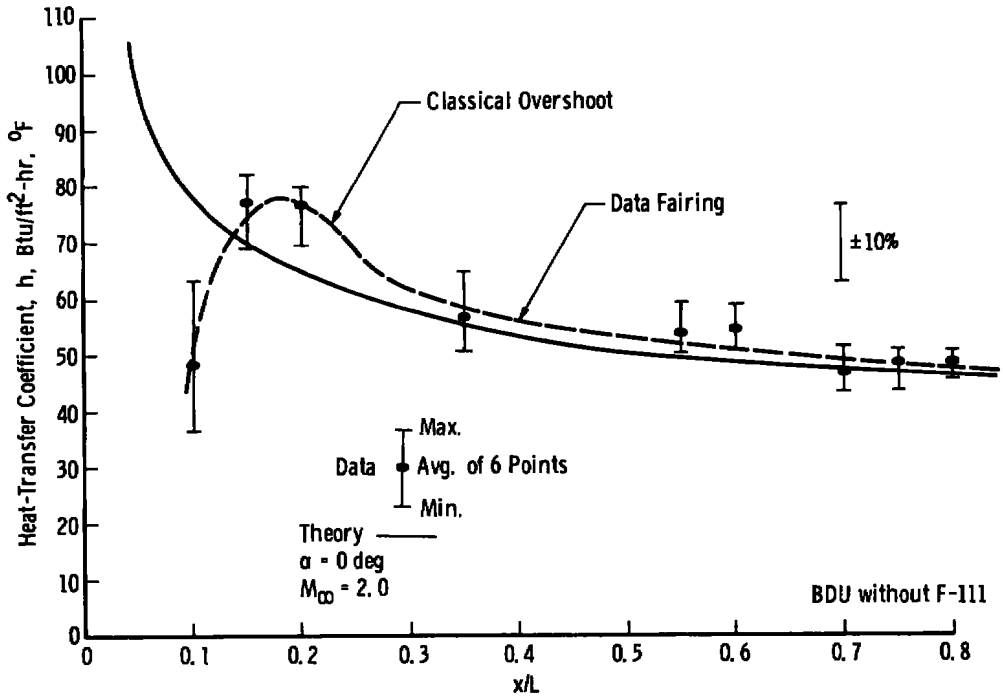


Figure 19. Undisturbed (interference-free) heat distributions on BDU model.

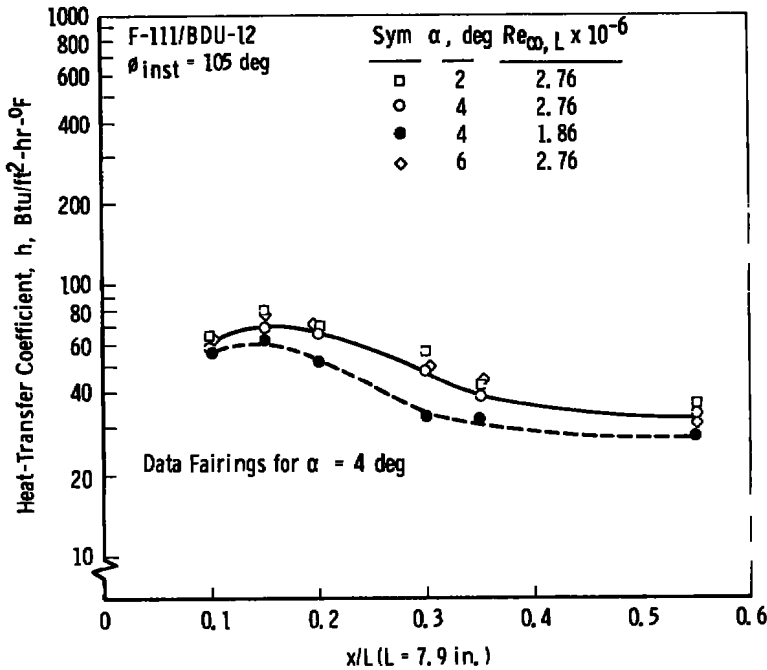
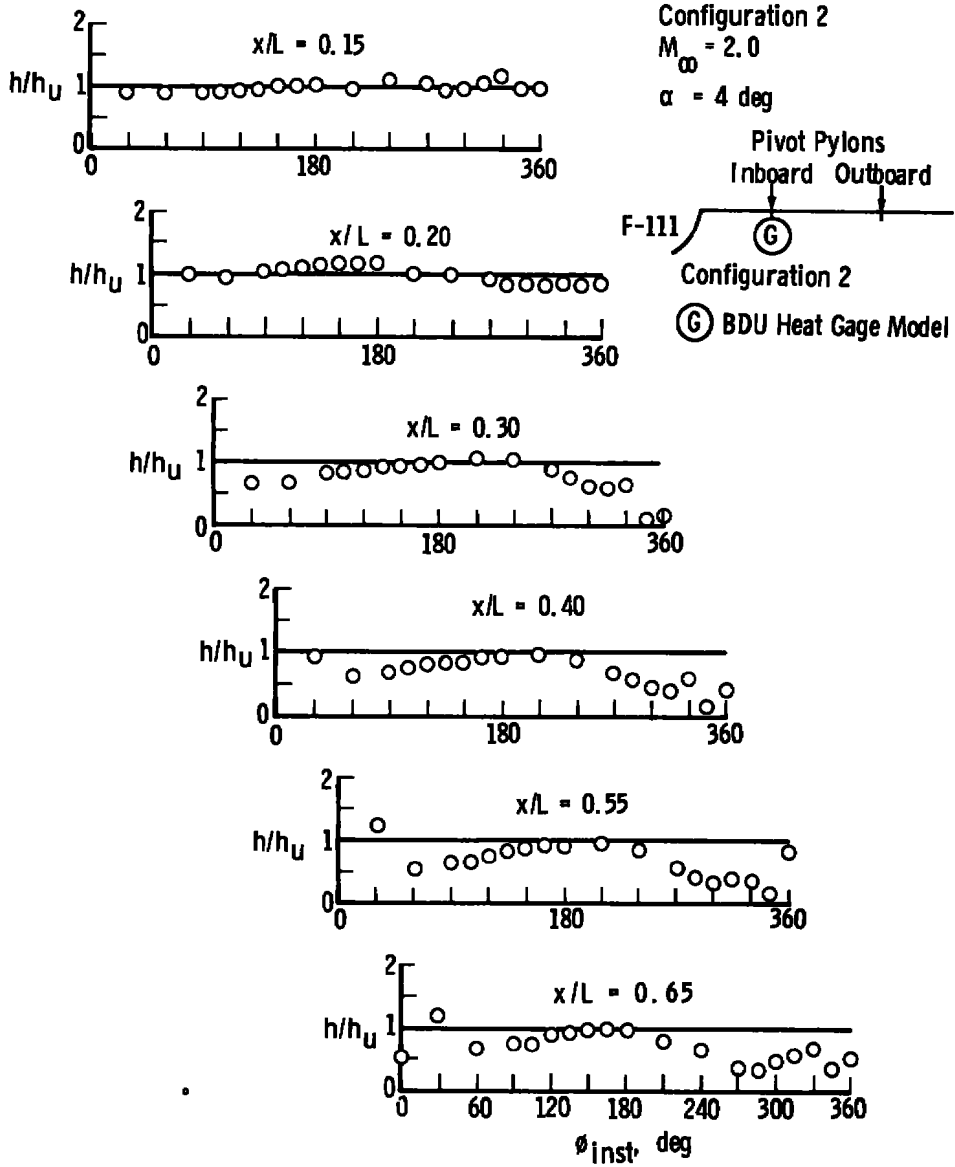
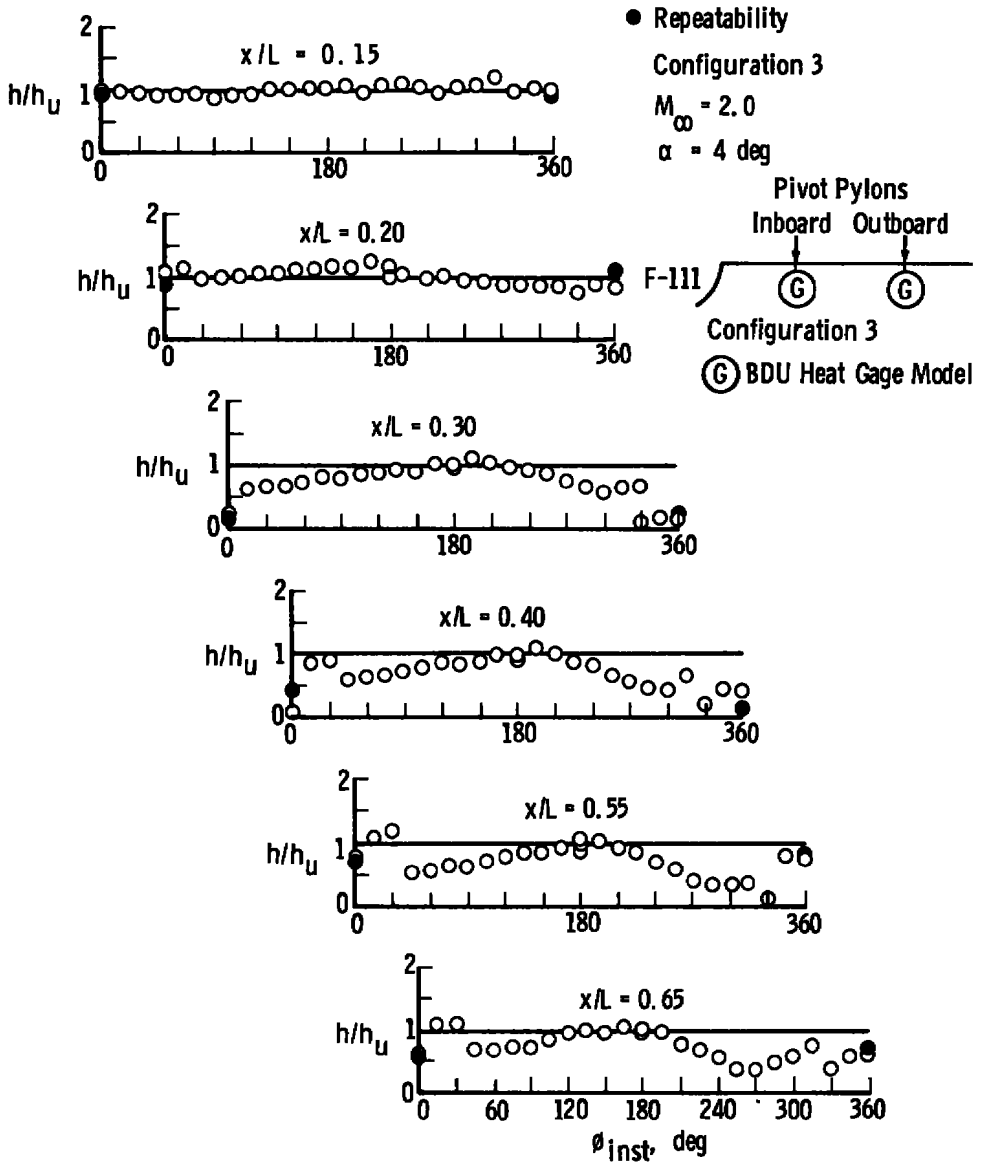


Figure 20. Heat-transfer results from wind tunnel (VKF/Tunnel A).

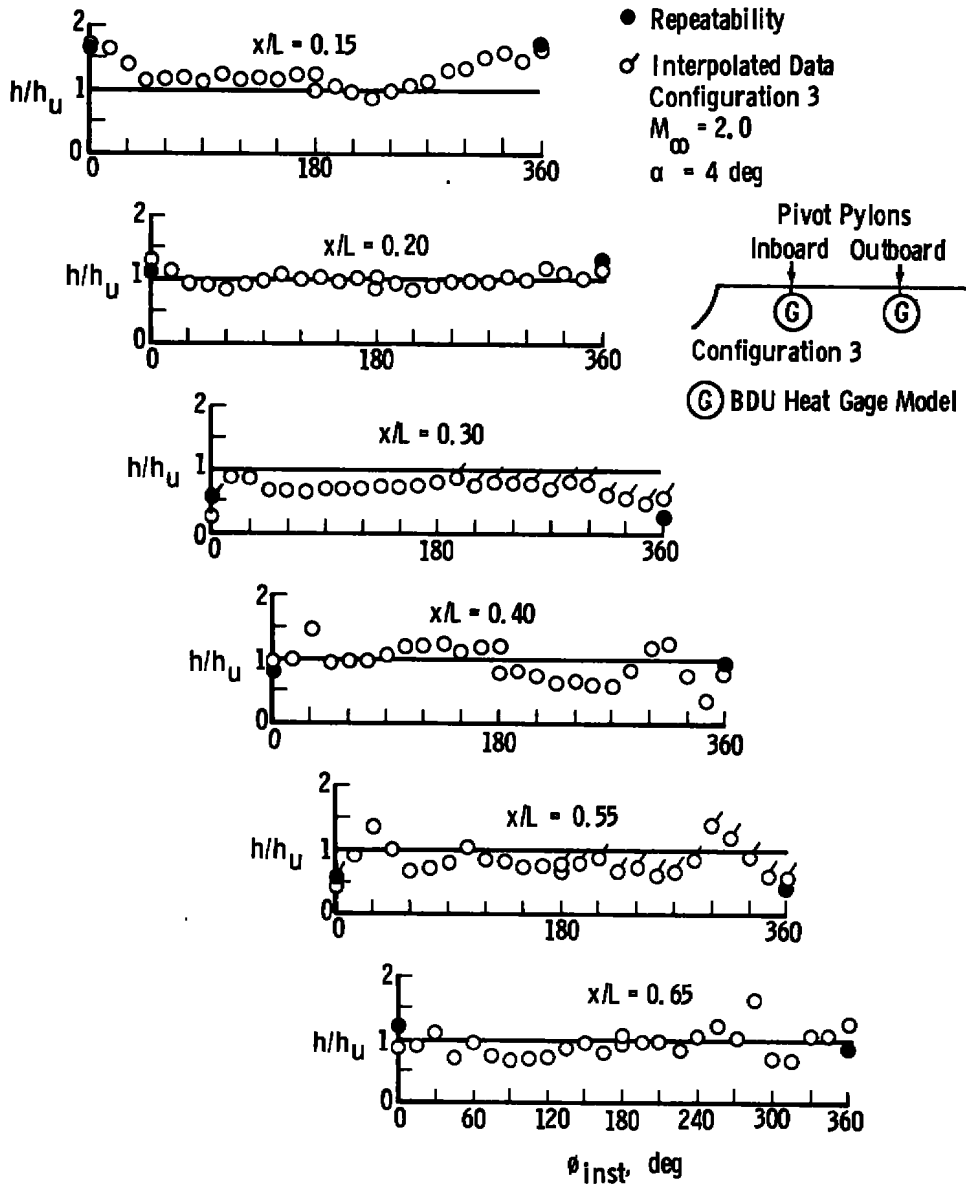


a. Inboard BDU

Figure 21. Circumferential heating distributions.

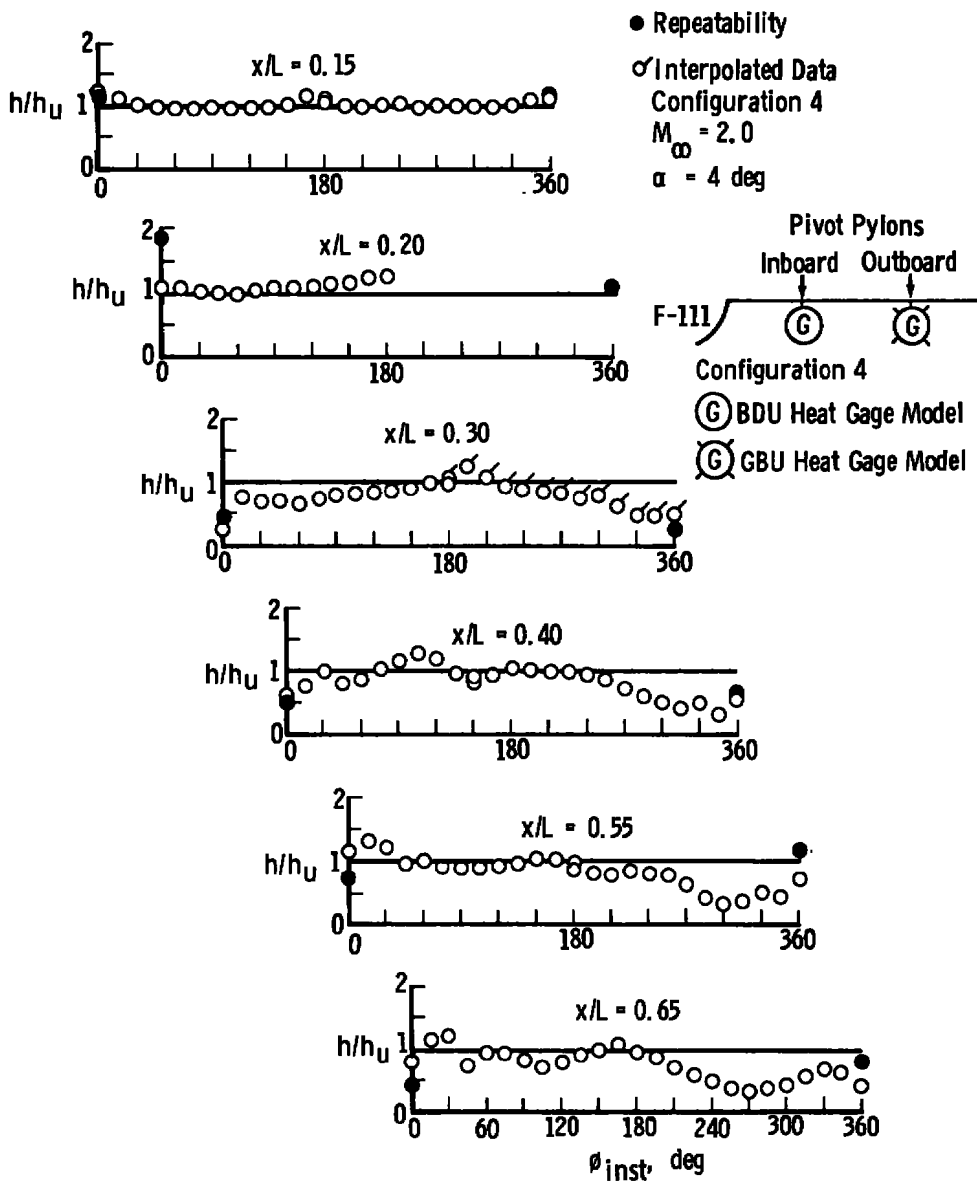


b. Inboard BDU with BDU on outboard pylon  
 Figure 21. Continued.

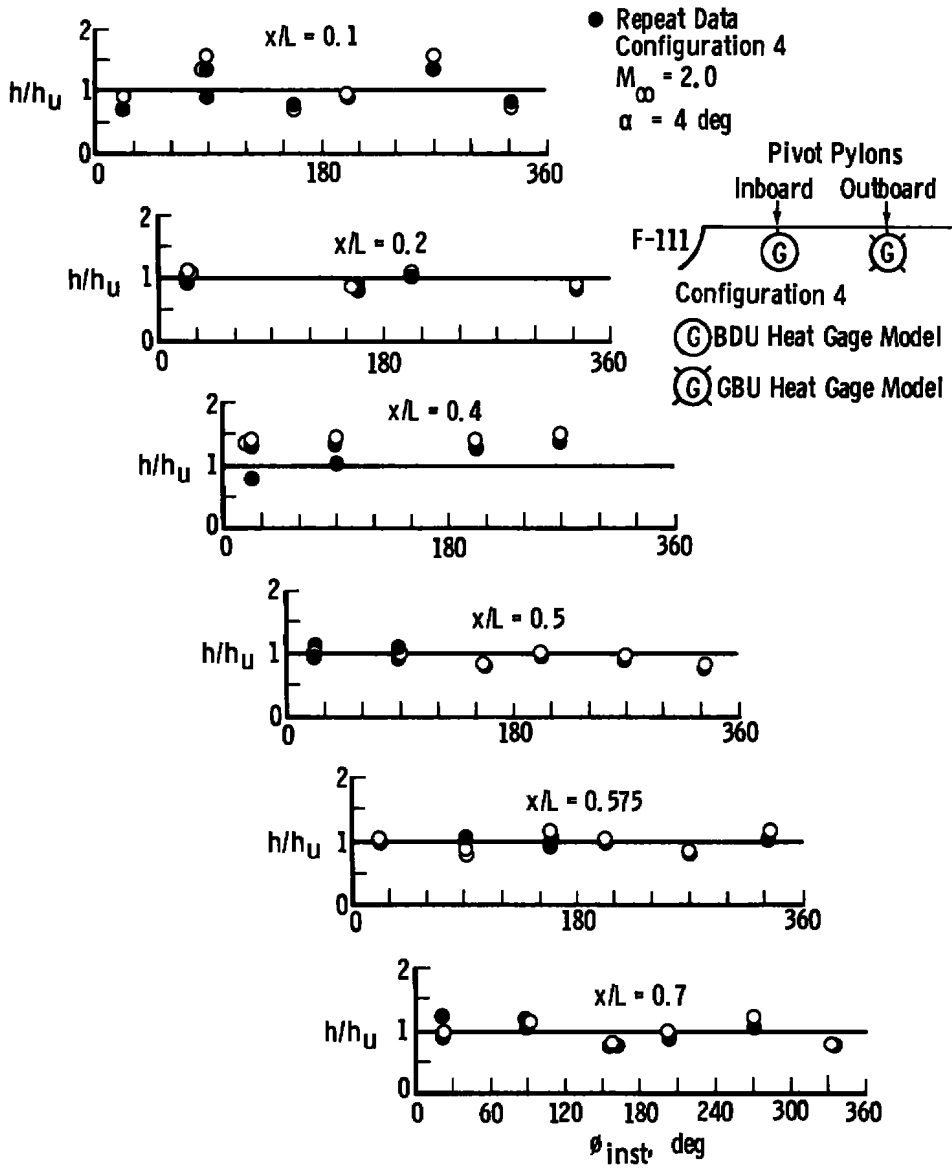


c. Outboard BDU with BDU on inboard pylon  
 Figure 21. Continued.

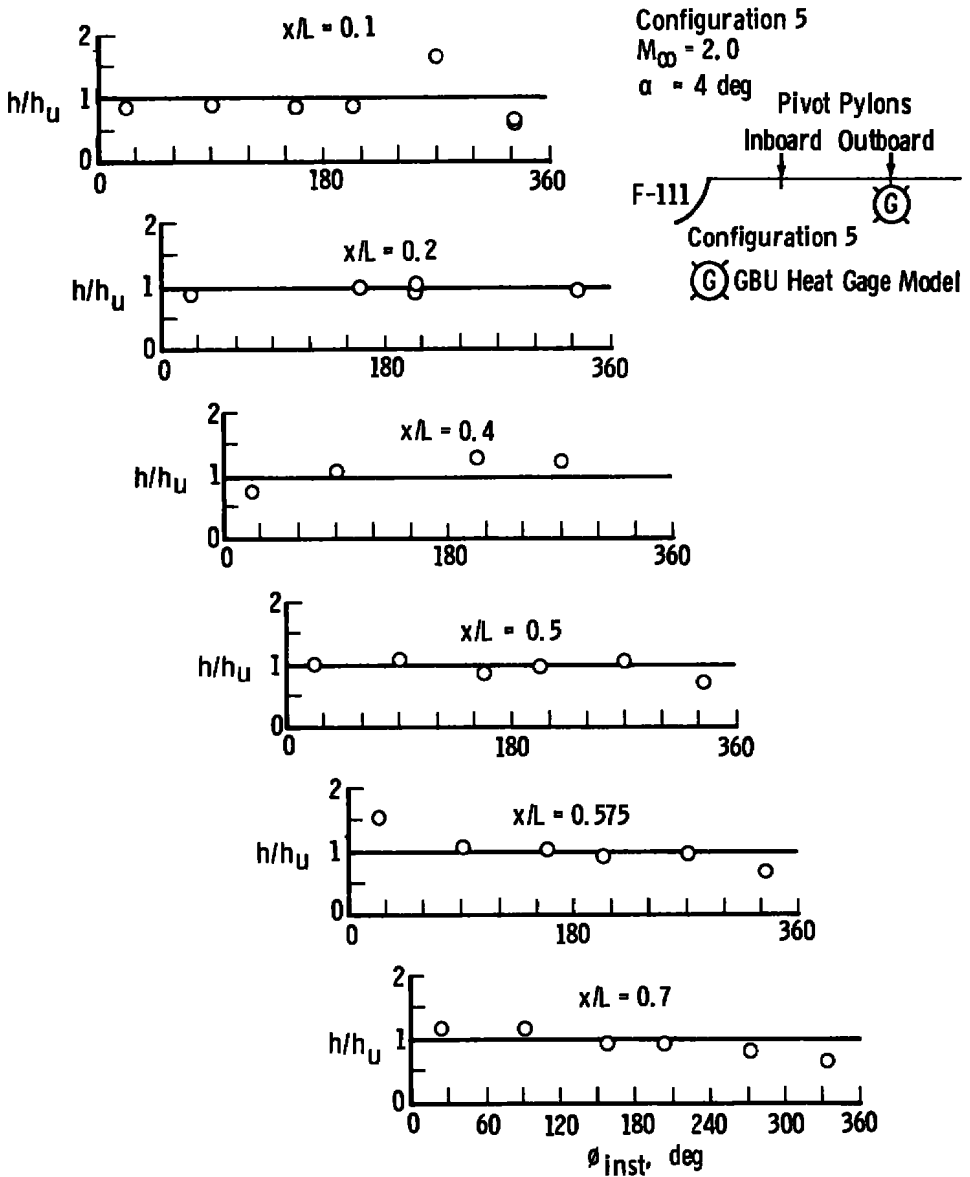




d. Inboard BDU with GBU on outboard pylon  
 Figure 21. Continued.



e. Outboard GBU with BDU on inboard pylon  
 Figure 21. Continued.



f. GBU on outboard pylon  
 Figure 21. Concluded.

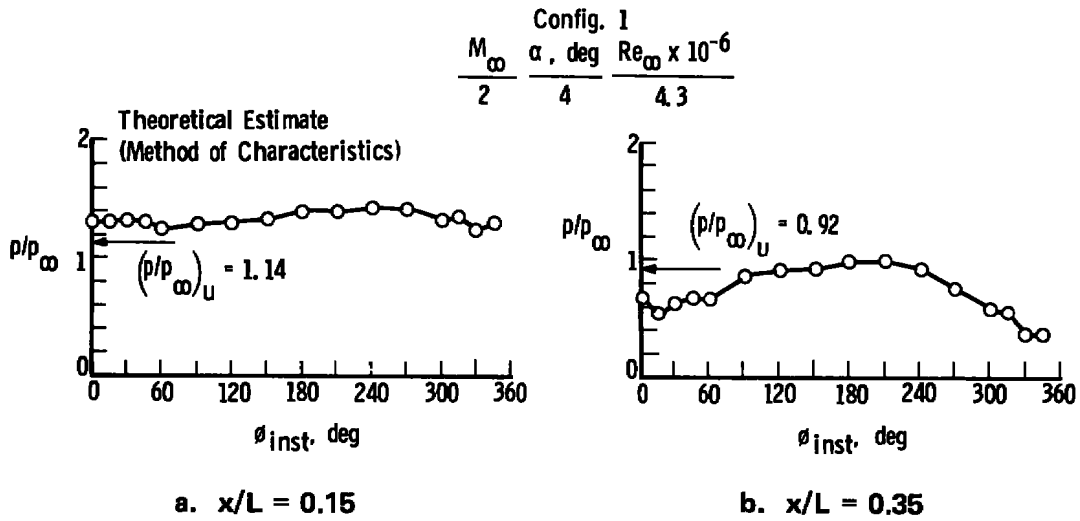


Figure 22. Circumferential pressure distributions on BDU model mounted on inboard pylon.

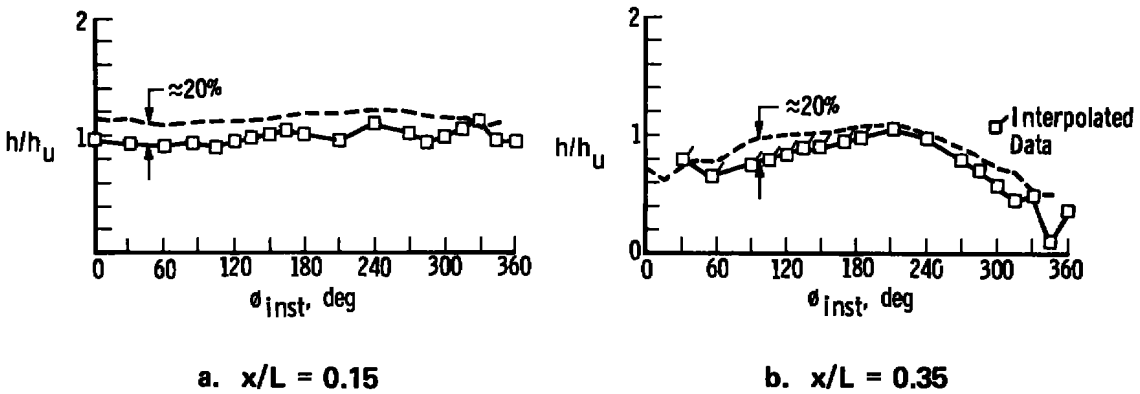
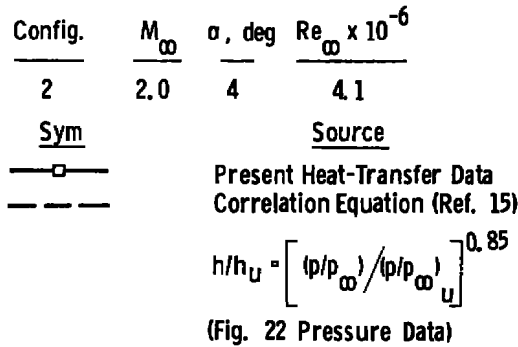


Figure 23. Comparison of measured and calculated interference heating distributions on BDU model mounted on inboard pylon.

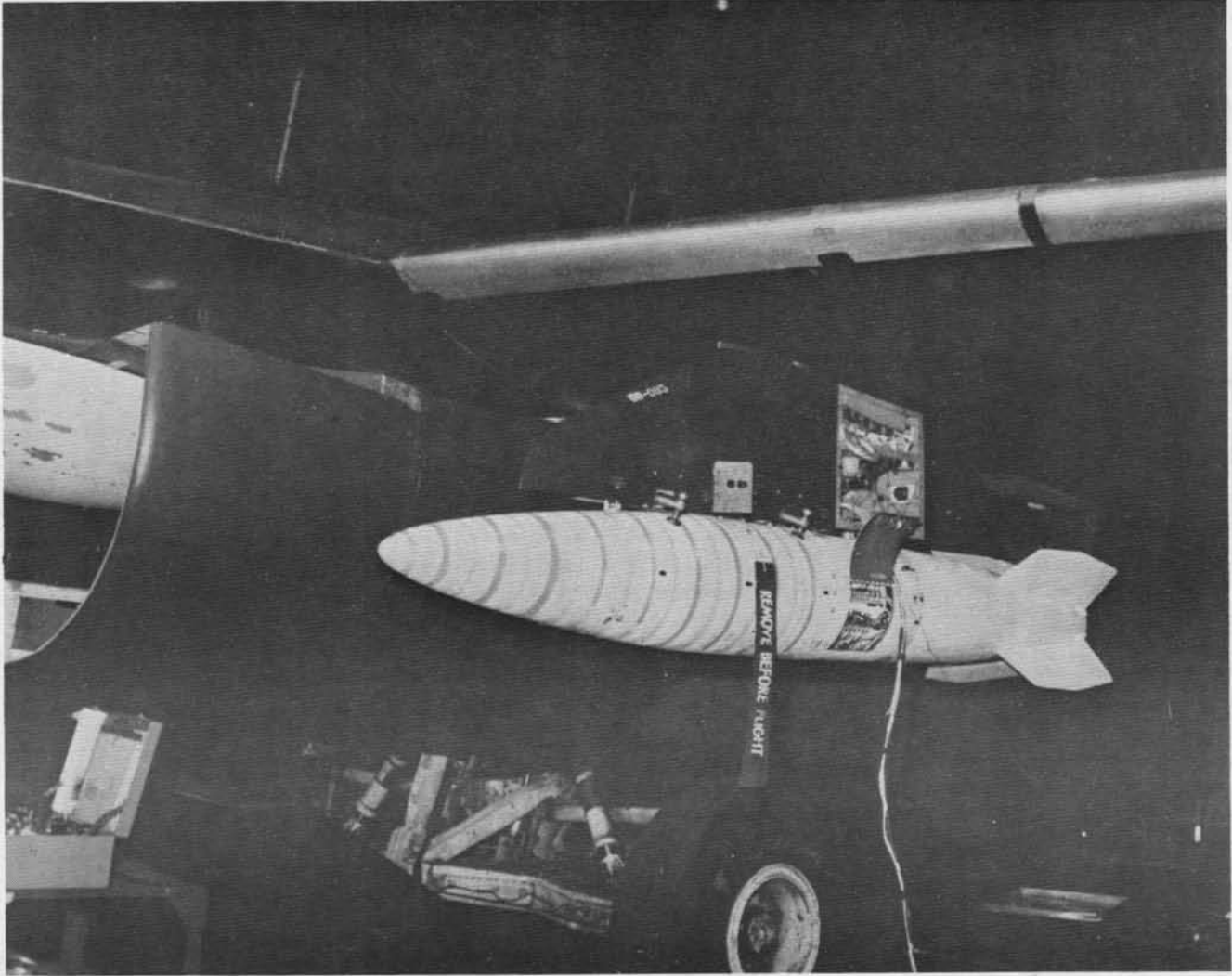


Figure 24. Pre-flight photograph of BDU with phase-change paint applied.

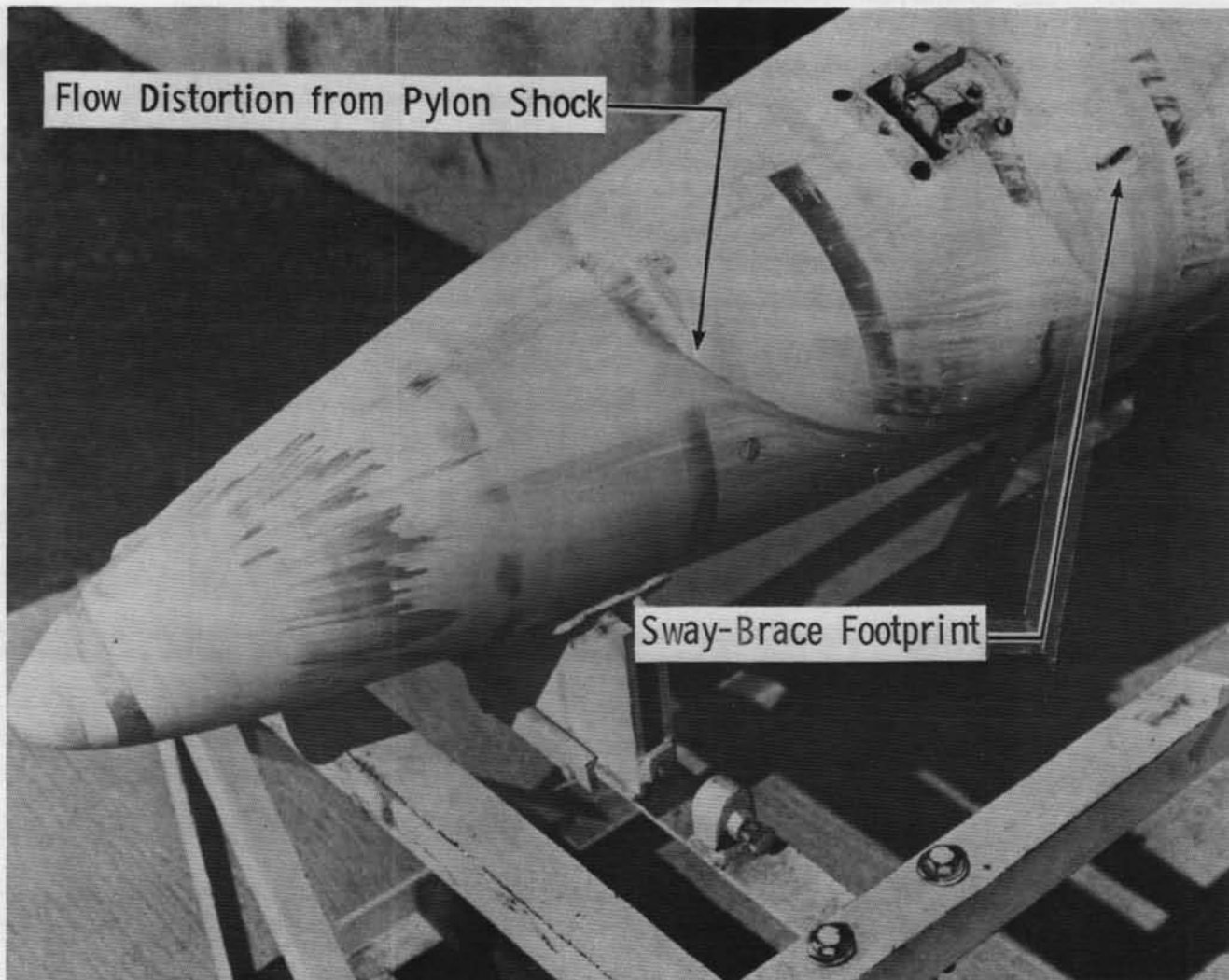
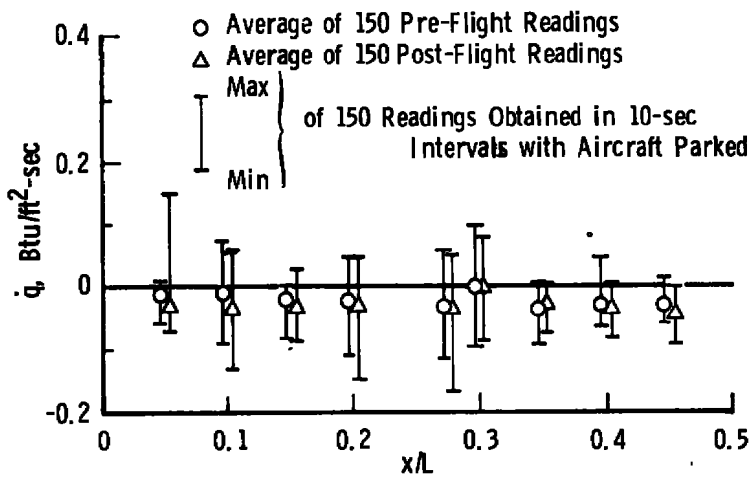
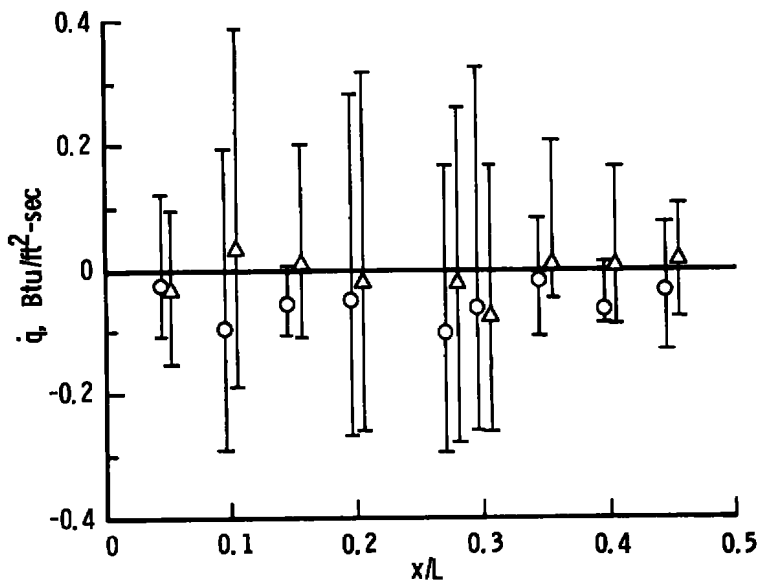


Figure 25. Post-flight photograph of phase-change paint after Mach 2.5 flight.



a. Flight 16



b. Flight 18

Figure 26. Illustrations of recorded  $\dot{q}$  variations (noise) with aircraft parked in hanger.

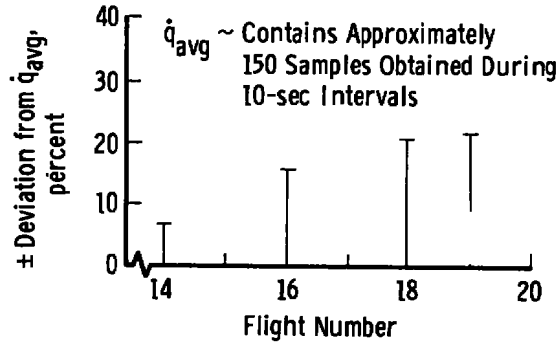


Figure 27. Illustration of relative "noise level" for flights.

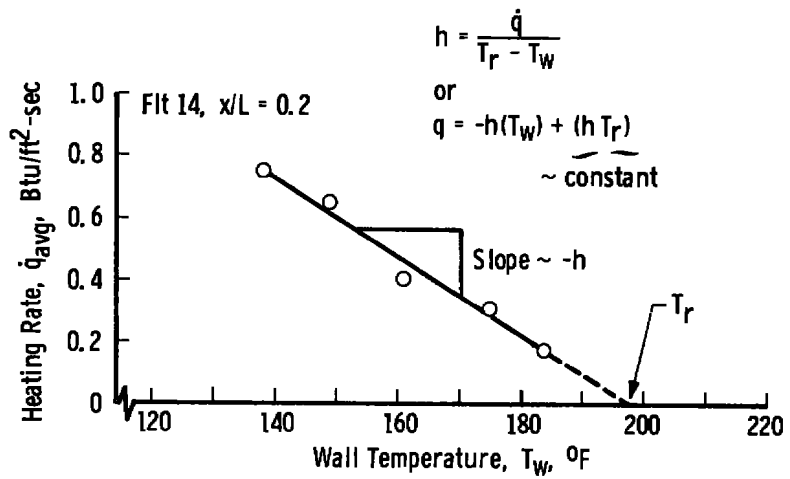


Figure 28. Illustration of data reduction technique (flight).



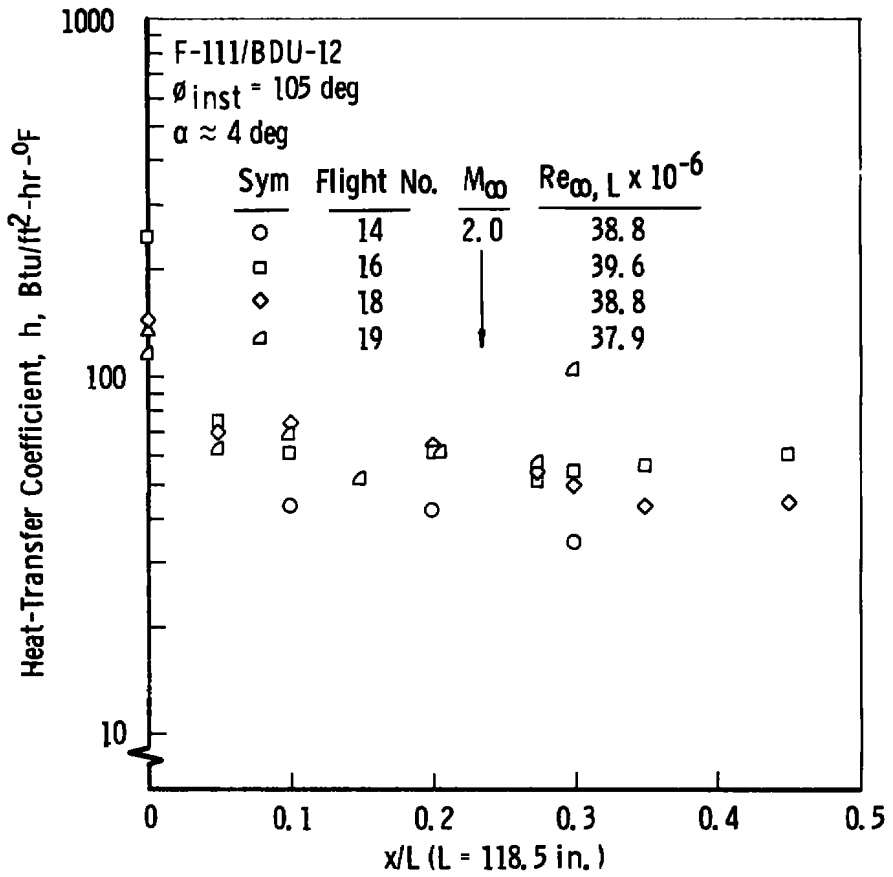


Figure 29. Heat-transfer results from flight test.

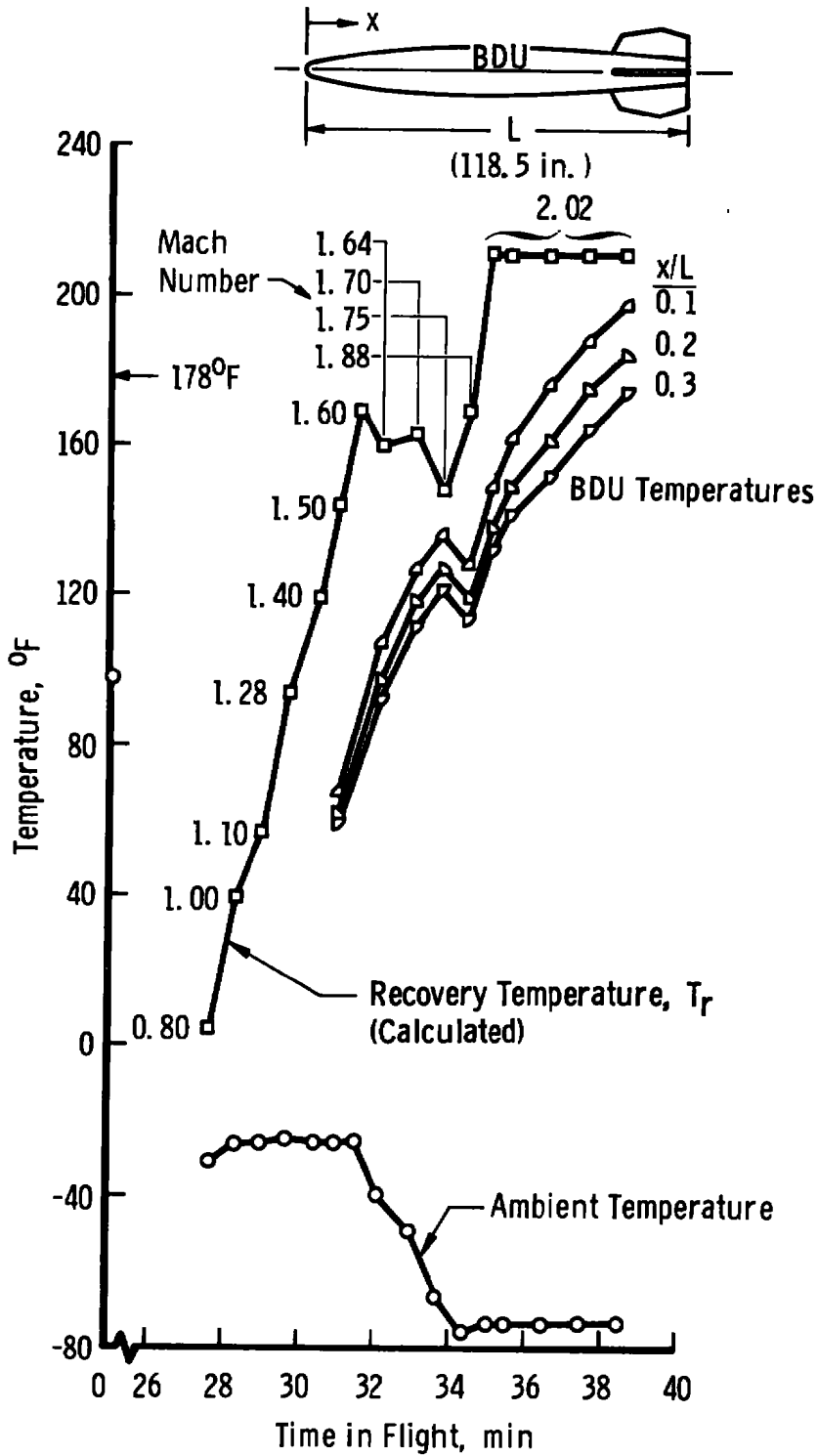


Figure 30. Principal results from flight test No. 14.

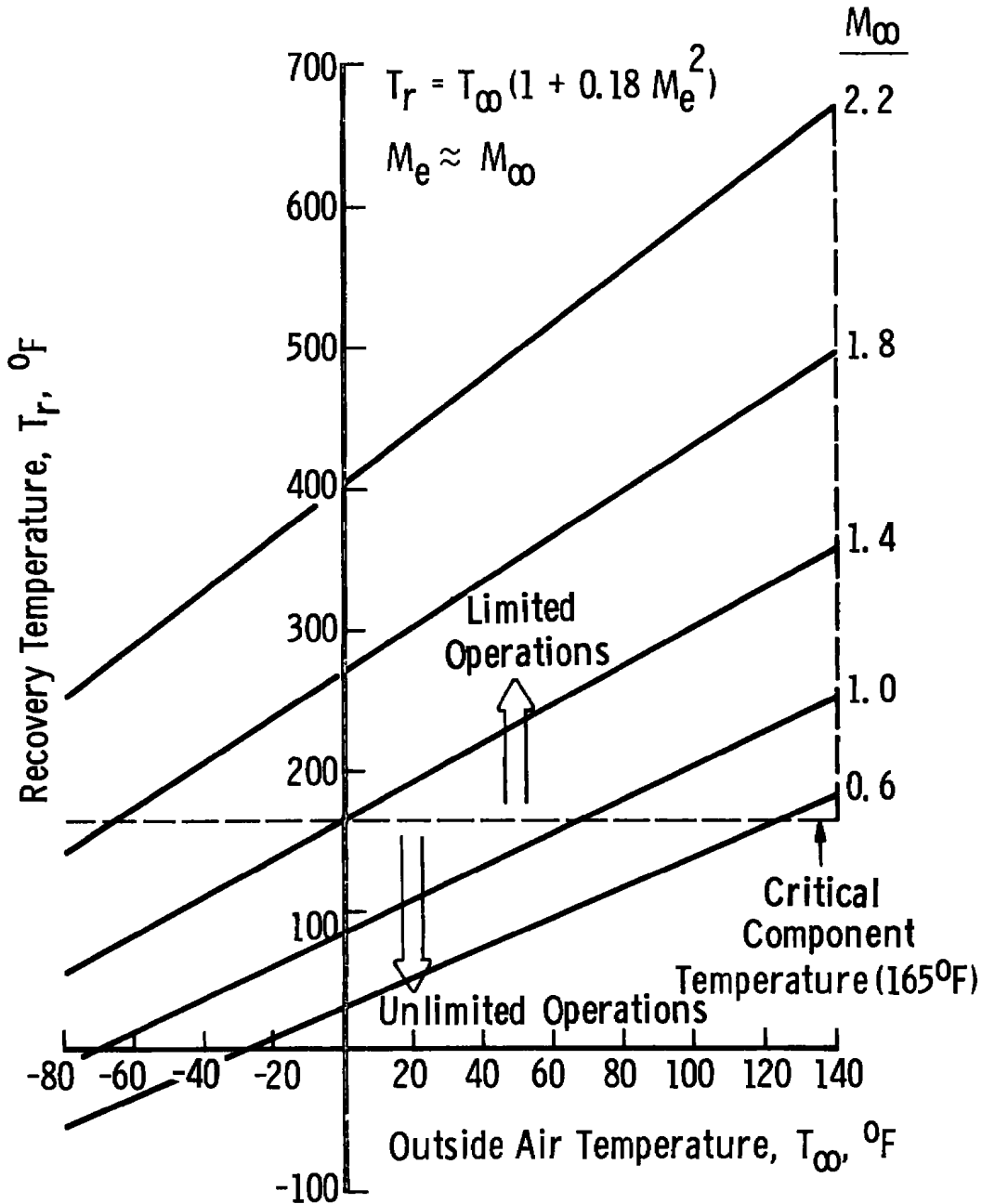


Figure 31. Illustration showing the importance of ambient temperatures on maximum possible store temperatures.

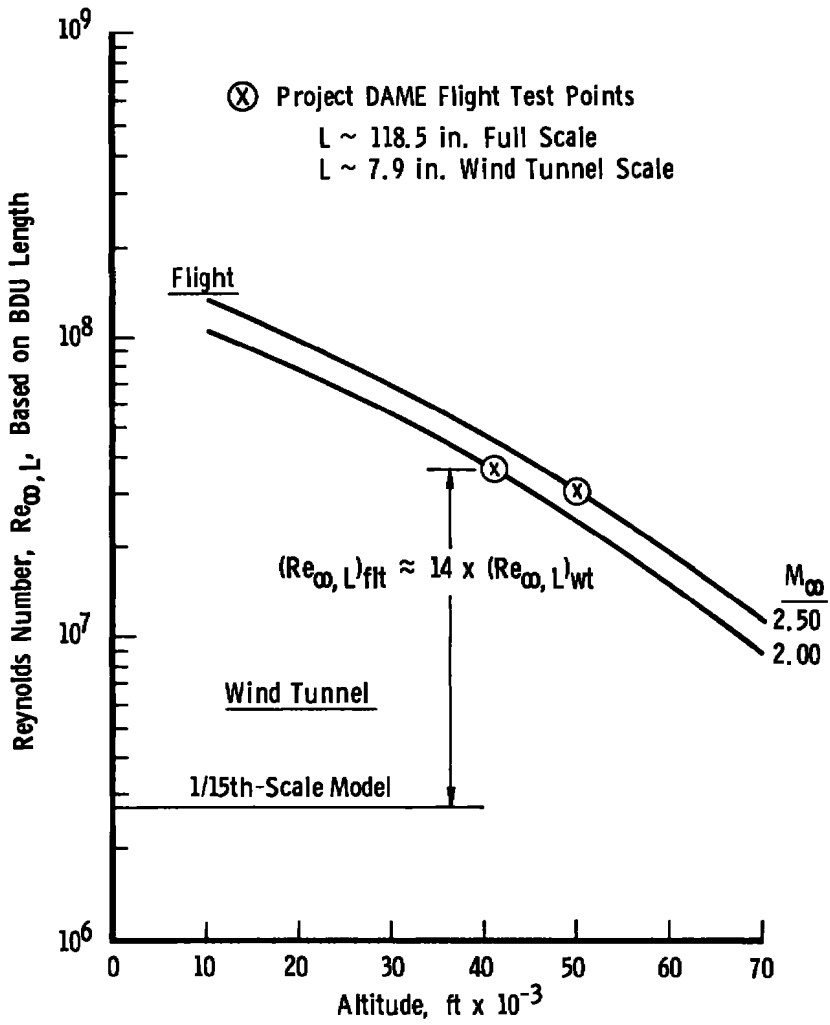


Figure 32. Comparison of wind tunnel and flight test Reynolds numbers.

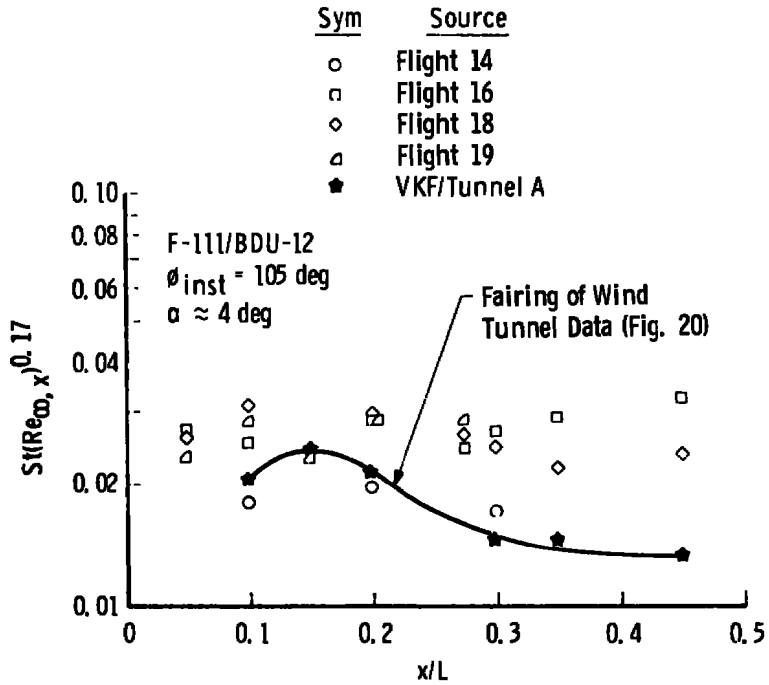


Figure 33. Comparison of flight test and wind tunnel results.

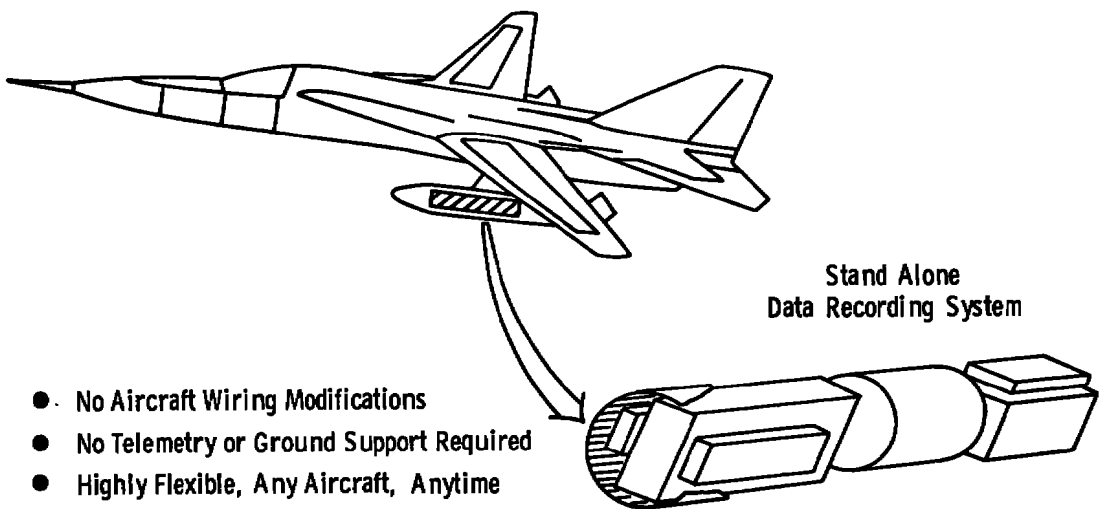


Figure 34. Sketch illustrating, stand-alone airborne data recording system.

**Table 1. Test Summary**

Configuration	Type Data	$M_\infty$	$Re_\infty \times 10^{-6} \text{ft}^{-1}$	Pitch, $\alpha$ , deg	$\theta_{inst}$ , deg
BDU (un-disturbed)	Heat-Transfer ↓	1.75	3.8	0	N/A ↓
		2.0	1.5, 2.8, 4.2	0, 2, 4, 6	
		2.5	5.0	0	
GBU (un-disturbed)	Heat-Transfer ↓	1.75	3.9	0	↓
		2.0	1.4, 2.3, 4.2	0	
		2.5	5.1	0	
1	Pressure ↓	1.75	3.8	0, 1, 2, 4, 6	0 → 360 ↓
		2.0	4.3	0, 1, 2, 4, 6	
		2.5	5.2	4	
2	Heat-Transfer, Oil Flow* ↓	1.75	3.8	1, 4	0 → 360 ↓
		2.0	2.8, 4.2	0, 1, 2, 4, 6	
		2.5	5.1	0, 4	
3	Heat-Transfer ↓	2.0	1.4, 2.4, 4.2	0, 4	↓
		2.5	5.1	0, 4	
4	↓	2.0	1.4, 4.2	0, 4	↓
		2.5	5.1	0, 4	
5	↓	2.0	4.1	0, 4	↓
		2.5	5.1	0, 4	

\*Tested at each Mach number with  $\alpha = 4$  deg

## NOMENCLATURE

AF	Amplification factor (see Eq. (9))
$A_0, A_1$	Coefficients in least-squares linear curve fit
$C_p$	Specific heat of air, 0.24 Btu/lbm $^{\circ}$ R
h	Heat-transfer coefficient (see Eq. (5)), Btu/ft $^2$ - $^{\circ}$ F-hr (or sec) as noted
L	BDU length (see Fig. 6), in.
M	Mach number
n	Exponent in correlation parameter (see Eq. (1))
p	Pressure, psf or psi as noted
$\dot{q}$	Heat-transfer rate, Btu/ft $^2$ -sec
$Re_{\infty}$	Free-stream unit Reynolds number, ft $^{-1}$
$Re_{\infty,L}$	Free-stream Reynolds number based on BDU length (118.5 in. for flight, 7.9 in. for wind tunnel)
$Re_{\infty,x}$	Reynolds number based on free-stream conditions and x.
St	Stanton number, $\dot{q}/\rho_{\infty}V_{\infty}C_p(T_r - T_w)$
T	Temperature, $^{\circ}$ F
$T_r$	Recovery temperature, $^{\circ}$ R or $^{\circ}$ F as noted
$T_w$	Model wall temperature, $^{\circ}$ R or $^{\circ}$ F as noted
$V_{\infty}$	Free-stream velocity, ft/sec
x	Longitudinal centerline distance from BDU nose (see Fig. 6), in.
$\alpha$	Angle of attack, deg
$\mu_{\infty}$	Free-stream viscosity, lbm/ft-sec
$\rho_{\infty}$	Free-stream density, slugs/ft $^3$ or lbm/ft $^3$

$\phi_{inst}$  Store instrumentation circumferential location measured outboard from vertical (see Fig. 14), deg

**SUBSCRIPTS**

- flt Flight conditions
- wt Wind tunnel conditions
- u Undisturbed or interference-free conditions
- $\infty$  Free-stream conditions
- o Stagnation or stilling chamber conditions
- e Boundary-layer edge conditions